Modeling miRNA-driven post-transcriptional regulatory signals by using exon-intron split analysis (EISA) in pigs

Emilio Mármol-Sánchez[1*], Susanna Cirera[2], Laura M. Zingaretti[3], Mette Juul Jacobsen[2], Yuliaxis Ramayo-Caldas[4], Claus B. Jørgensen[2], Merete Fredholm[2], Tainã Figueiredo Cardoso[1†], Raquel Quintanilla[4], Marcel Amills[1,5]

[1]Centre for Research in Agricultural Genomics (CRAG), CSIC-IRTA-UAB-UB, Universitat Autònoma de Barcelona, 08193 Bellaterra, Spain.

[2]Department of Veterinary and Animal Sciences, Faculty of Health and Medical Sciences, University of Copenhagen, 1871 Frederiksberg C, Denmark.

[3]Universidad Nacional de Villa María, Villa María, Córdoba, Argentina.

[4]Animal Breeding and Genetics Program, Institute for Research and Technology in Food and Agriculture (IRTA), Torre Marimon, 08140 Caldes de Montbui, Spain.

[5]Departament de Ciència Animal i dels Aliments, Universitat Autònoma de Barcelona, 08193 Bellaterra, Barcelona, Spain.

*Emilio Mármol-Sánchez current address: Stockholm University, The Wenner-Gren Institute, Department of Molecular Biosciences, SciLifelab.

[†]Tainã Figueiredo Cardoso current address: Embrapa Pecuária Sudeste, Empresa Brasileira de Pesquisa Agropecuária (EMBRAPA), 13560-970, São Carlos, SP, Brazil.

Corresponding author: Emilio Mármol-Sánchez. Stockholm University, The Wenner-Gren Institute, Department of Molecular Biosciences, SciLifelab. Email: emilio.marmol.sanchez@gmail.com

Abstract

Bulk sequencing of RNA transcripts has typically been used to quantify gene expression levels and regulatory signals in different experimental systems. However, linking differentially expressed (DE) mRNA transcripts to gene expression regulators, such as miRNAs, remains challenging, as miRNA-mRNA interactions are commonly identified *post hoc* after selecting sets of genes of interest, thus biasing the interpretation of underlying gene regulatory networks.

In this study, we aimed at disentangling miRNA-driven post-transcriptional signals linked to porcine muscle and adipose tissue energy homeostasis. To this end, we performed an exon-intron split analysis (EISA) to muscle and fat RNA-seq data from two Duroc pig populations. One of these populations was subjected to fasting-feeding conditions, while the other one represented divergent fatness profiles. After running EISA, protein-coding mRNA genes with downregulated exonic fractions and high post-transcriptional signals were significantly enriched for binding sites of DE upregulated miRNAs. Moreover, these downregulated genes showed an increased expression covariation for the exonic fraction compared to that of the intronic fraction. On the contrary, they did not show enrichment for binding sites of non-DE highly expressed or downregulated DE miRNAs. Among the set of loci displaying miRNA-driven post-transcriptional regulatory signals, we observed genes related to glucose homeostasis (*DKK2*, *PDK4*, *IL18*, *NR4A3*, *CHRNA1*, *TET2*), cell differentiation (*PBX1*, *BACH2*) or adipocytes metabolism (*SESN3*, *ESRRG*, *SAMD4*, *LEP*, *PTGFR*, *SERPINE2*, *RNF157*, *GPLD1*, *NCF2*, *OSBPL10*, *PRSS23*). Our results highlighted mRNA genes showing post-transcriptional miRNA-driven downregulation by using exonic and intronic fractions of RNA-seq datasets from muscle and adipose tissues in pigs.

Keywords: Exon-intron split analyses, microRNA, pigs, energy homeostasis.

1. Introduction

Messenger RNA (mRNA) expression and turnover in the cell metabolism are subjected to complex yet poorly characterized regulatory mechanisms that contribute to shaping fine-tuned biological responses to different stimuli [1]. Cellular metabolic changes are hence a direct manifestation of intricate interactions between expressed transcripts and other regulatory elements that modify their abundance, localization, fate and degradation rate. MicroRNAs (miRNAs) are primarily engaged in the post-transcriptional control of gene expression through inhibition of translation and/or destabilization of target mRNAs by poly(A) shortening and subsequent degradation [2]. Changes in the abundance of mRNAs targeted by miRNAs can be inferred through the analysis of covariation patterns. Such approach can help to unravel direct or indirect molecular interactions connecting and regulating biological pathways.

In order to disentangle regulatory functions driven by miRNAs, researchers typically focus on specific sets of genes of their interest showing significant expression changes and harboring binding sites for DE miRNAs [3–9]. This approach, however, is biased by the fact that genes are selected after differential expression analysis and also by the performance of an *ad hoc* search of predicted interactions between the 3'-UTRs of mRNAs and the seed regions of miRNAs. Besides, one of the main limitations of differential expression analysis is that it does not discriminate whether changes in expression take place either at the transcriptional or post-transcriptional levels. Such distinction is essential to understand at which level or levels of the mRNA life cycle the regulation is taking place.

To address this issue, Gaidatzis *et al*. [10] devised a methodology denominated as exon-intro split analysis (EISA), which separates the transcriptional and post-transcriptional components of gene regulation by considering that intronic reads are mainly derived

from heterogeneous nuclear RNAs (unprocessed mRNAs or pre-mRNAs) and consequently represent the magnitude of the transcriptional component. Such assumption is based on early reports describing intronic expression as a proxy of nascent transcription and co-transcriptional splicing events [11–13].

On the other hand, Gaidatzis *et al.* [10] proposed that the magnitude of the post-transcriptional component can be deduced by comparing the amounts of exonic and intronic reads [10]. For instance, if a gene shows similar levels of intronic reads in two different states but a strong downregulation of exonic reads after applying a certain treatment or challenge (nutrition, infection, temperature etc.), this could be indicative of an induced inhibition by a post-transcriptional regulatory factor [10,14,15].

A high number of differential expression studies have been performed in pigs during the last decade [16–24], but to the best of our knowledge in none of these studies the transcriptional and post-transcriptional components of gene regulation have been discriminated. In the present study, we aimed to dissect the contribution of miRNAs to post-transcriptional regulation in pigs by using the EISA methodology. To do so, we have used two different experimental models, i.e., muscle samples from Duroc pigs before and after food intake and adipose tissue samples from Duroc-Göttingen minipigs with divergent fatness profiles.

2. Materials and methods

2.1. Experimental design, sampling and processing

The contribution of miRNAs to post-transcriptional regulation in pigs has been investigated in two different experimental systems:

(i) Duroc pigs: Twenty-three gilts divided in two fasting/feeding regimes, i.e. 11 gilts (*AL-T0*) slaughtered in fasting conditions and 12 gilts (*AL-T2*) slaughtered immediately after 7 h with access to *ad libitum* feed intake [7,22,25]. Immediately after slaughtering, *gluteus medius* (GM) skeletal muscle samples were collected and snap-frozen at -80°C.

(ii) Duroc-Göttingen minipig F_2 inter-cross: Ten individuals with divergent fatness profiles for their body mass index (BMI) metric (5 *lean* and 5 *obese*) were selected from the UNIK resource population [26,27], as described in Jacobsen et al. 2019 [28]. Tissue samples from retroperitoneal tissue of each animal were collected and mature adipocytes were isolated following the protocol of Decaunes et al. 2011 [29] with modifications reported in [28].

Further details about RNA-seq and small RNA-seq expression data generated from both experimental designs have been previously described [7,22,28]. In brief, total RNA was isolated from GM tissue using the RiboPure kit (Ambion, Austin, TX). Total RNA was also isolated from adipocytes following the protocol of Cirera 2013 [30]. Sequencing libraries were prepared with dedicated TruSeq stranded total RNA kits (Illumina Inc. CA) [7,28] and paired-end sequenced in a HiSeq 2000 equipment (Illumina Inc. CA). Small RNA-specific libraries were prepared from total RNA isolates by using the TruSeq Small RNA Sample Preparation Kit (Illumina Inc., CA). Single-end (1 x 50 bp) sequencing of the small RNA fraction was carried out in a HiSeq 2500 equipment (Illumina Inc., CA).

Sequencing reads generated in the RNA-Seq and small RNA-Seq experiments concerning fast and fed Duroc gilts, as well as lean and obese Duroc-Göttingen minipigs, were trimmed to remove any remaining sequencing adapters with the Cutadapt software [31]. Reads were mapped against the Sscrofa11.1 porcine assembly [32] with the HISAT2 aligner [33] and default parameters for RNA-Seq reads. In

125 contrast, the Bowtie Alignment v.1.2.1.1 software [34] with small sequence reads
126 specifications (*bowtie -n 0 -l 25 -m 20 -k 1 --best --strata*) was used to align small RNA-
127 Seq reads to the Sscrofa11.1 porcine reference assembly [32].
128
129 **2.2. Exon/Intron quantification**
130 We generated exonic and intronic-specific annotations spanning all genes available
131 using the gtf formatted Sscrofa.11.1 v.103 gene annotation file retrieved from Ensembl
132 repositories (http://ftp.ensembl.org/pub/release-103/gtf/sus_scrofa/). Overlapping
133 intronic/exonic regions, as well as singleton positions were removed [35]. Each intronic
134 region was trimmed by removing 10 nucleotides in both sides to avoid exonic reads
135 mapping close to exon/intron junctions. We then used the featureCounts function
136 included in the Rsubread package [36] to quantify gene expression profiles based on
137 exonic and intron expression patterns for each gene, independently. MiRNA expression
138 profiles were estimated using the Sscrofa11.1 v.103 mature miRNA annotation with the
139 featureCounts software tool [37] in single-end mode and with default parameters.
140
141 **2.3. Exon/intron split analysis (EISA).**
142 We applied EISA to differentiate gene expression regulation based on post-
143 transcriptional effects [10,14,15]. To this end, we separately estimated the exonic and
144 intronic abundance of each annotated mRNA gene using the Sscrofa11.1 v.103
145 exon/intron custom annotation generated as described in the previous section. Only
146 genes showing average expression values above 1 count-per-million (CPM) in at least
147 50% of animals were retained for further analyses.
148 Normalization was performed independently for exon and intron counts by multiplying
149 each i^{th} gene expression in each j^{th} sample by the corresponding mean gene expression

and dividing by the total number of quantified counts per sample [10]. Exonic and intronic gene abundances were subsequently transformed to a $\log_2$ scale, adding a pseudo-count of 1 and averaged within each considered treatment groups (*AL-T0* and *AL-T2* for GM tissues and *lean* and *obese* for adipocyte isolates).

Only genes with successful exonic and intronic quantified read counts were considered in our analyses. The transcriptional component (Tc) contribution to the observed differences in each i^{th} gene was expressed as the increment of intronic counts in fed (*AL-T2*) and *obese* animals with respect to fasting (*AL-T0*) and *lean* animals ($\Delta Int = Int_{2i} - Int_{1i}$), respectively. The increment of exonic counts (ΔEx) was also calculated, and the post-transcriptional component (PTc) effect was expressed as $\Delta Ex - \Delta Int = (Ex_{2i} - Ex_{1i}) - (Int_{2i} - Int_{1i})$. Both components were z-scored to represent comparable ranges between ΔEx and ΔInt estimates. All implemented analyses have been summarized in **Fig. S1**. A ready-to-use modular pipeline for running EISA is publicly available at https://github.com/emarmolsanchez/EISACompR.

2.4. Post-transcriptional signal prioritization

In order to obtain a prioritized list of genes showing relevant signals of post-transcriptional regulation, the top 5% genes with the highest negative PTc scores were retrieved. We only focused on genes showing strongly reduced exonic fraction (ΔEx) values of at least 2-folds for post-transcriptional signals in *AL-T0* vs *AL-T2* and in *lean* vs *obese* animals.

2.5. Differential expression analyses and significance of PTc scores

Differential expression analyses were carried out with the *edgeR* package [38] by considering the exonic fraction of mRNAs, as well as miRNA expression profiles from

RNA-Seq and small RNA-Seq data sets corresponding to the wo experimental systems under study. Expression filtered raw counts for exonic reads were normalized with the trimmed mean of M-values normalization (TMM) method [39] and the statistical significance of mean expression differences was tested with a quasi-likelihood F-test [38]. Correction for multiple hypothesis testing was implemented with the Benjamini-Hochberg false discovery rate approach [40]. Messenger RNAs were considered as differentially expressed (DE) when the absolute value of the fold-change (FC) was higher than 2 ($|FC| > 2$) and q-value < 0.05. For miRNAs, $|FC| > 1.5$ and q-value < 0.05 were used instead. The statistical significance of the post-transcriptional (PTc) component was evaluated by incorporating the intronic quantification as an interaction effect for exonic abundances [10].

2.6. miRNA target prediction

Putative interactions between the seed regions of expressed miRNAs (small RNA-seq datasets) and the 3'-UTRs of expressed protein-coding mRNA genes (RNA-seq datasets) were predicted on the basis of sequence identity using the Sscrofa11.1 reference assembly. The annotated 3'-UTRs from porcine mRNAs were retrieved from the Sscrofa11.1 v.103 available at BioMart (http://www.ensembl.org/biomart) and miRBase [41] databases. The 3'-UTR sequences shorter than 30 nts were discarded. Redundant seeds from mature porcine microRNAs were removed. The seedVicious v1.1 tool [42] was used to infer miRNA-mRNA interactions. MiRNA-mRNA 8mer, 7mer-m8 and 7mer-A1 interactions were considered as the most relevant among the full set of canonical and non-canonical interactions [2,43,44].

Following early reports about the relationship between miRNA binding site context and miRNA-mRNA interaction efficacy [43], the *in silico*-predicted miRNA-mRNA

interactions matching any of the following criteria were removed: (i) Binding sites are located in 3'-UTRs at less than 15 nts close to the end of the open reading frame (and the stop codon) or less than 15 nts close to the terminal poly(A) tail, (ii) binding sites are located in the middle of the 3'-UTR in a range comprising 45-55% of the central region of the non-coding sequence and (iii) binding sites lack AU-rich elements in their immediate upstream and downstream flanking regions comprising 30 nts each.

Covariation patterns between miRNAs and their predicted mRNA targets were assessed by computing Spearman´s correlation coefficients (ρ) with the TMM normalized and $\log_2$ transformed expression profiles of the exonic fractions of mRNA and miRNA genes. To determine the contribution of miRNAs to post-transcriptional regulation in the two experimental systems under study, only miRNA-mRNA predicted pairs comprising DE upregulated miRNAs (FC > 1.5; *q*-value < 0.05) and mRNA genes with relevant PTc scores (see post-transcriptional signal prioritization section) were taken into consideration.

2.7. miRNA target enrichment analyses

We sought to determine if the overall number of mRNA genes with high post-transcriptional signals (the ones with the top 5% negative PTc scores and reduced ΔEx values > 2-folds) were significantly enriched to be targeted by at least one upregulated miRNA (FC > 1.5; *q*-value < 0.05), compared with the whole set expressed mRNAs genes with available 3'-UTRs from both *AL-T0* vs *AL-T2* and *lean* vs *obese* datasets. Enrichment analyses were carried out using the Fisher's exact test implemented in the *fisher.test* R function. Results were considered significant when the nominal *P*-value < 0.05.

We also tested whether these genes were enriched for binding sites of the top 5% most highly expressed miRNA genes, excluding significantly upregulated miRNAs, as well as for binding sites of significantly downregulated miRNAs (FC < -1.5; *q*-value < 0.05). Given the relatively low statistical significance of DE miRNAs observed in the UNIK Duroc-Göttingen minipigs (l*ean* vs *obese*), we considered that miRNAs were significantly upregulated in this particular data set when FC >1.5 and *P*-value < 0.01. Further details can be found in **Supplementary Methods File S1**.

2.8. Gene covariation network and covariation enrichment score

We computed pairwise correlation coefficients among the whole set of DE mRNA genes in the *AL-T0* vs *AL-T2* (*q*-value < 0.05, N = 454) and *lean* vs *obese* (*q*-value < 0.05, N = 299) experimental contrasts. These correlations were compared with those corresponding to the set of genes with relevant post-transcriptional signals and putatively targeted by DE upregulated miRNAs. Normalized exonic and intronic estimates in the $\log_2$ scale obtained from EISA analyses were used to compute Spearman's correlation coefficients (ρ) for each potential pair of DE mRNA genes plus those with post-transcriptional signals but without significant DE. Self-correlation pairs were excluded. Significant covariation events were identified with the Partial Correlation with Information Theory (PCIT) network inference algorithm [45] implemented in the *pcit* R package [46]. Non-significant covarying pairs were set to zero, while a value of 1 was assigned to significant covarying pairs with both positive or negative coefficients $|\rho| > 0.6$.

The potential contribution of miRNAs to shape the observed covariation patterns was assessed by calculating a covariation enrichment score (CES) following Tarbier et al. 2020 [47]. Significant differences among the set of exonic, intronic and control CES

values were tested with a non-parametric approach using a Mann-Whitney U non-parametric test [48]. Further details about CES calculation and implementation can be found in **Supplementary Methods File S1**.

2.9. Estimating the expression levels of miRNAs and several of their predicted mRNA targets by qPCR

Retroperitoneal adipose tissue (~20 ml) was taken from the abdominal cavity of UNIK intercrossed Duroc-Göttingen minipigs pigs quickly after slaughtering (more details about UNIK minipig population are described in [26,27]). Adipocyte cells from adipose tissue where isolated as described in Jacobsen et al. 2019 [28] and RNA was extracted following the method of Cirera (2013) [30]. Total RNA from adipocytes was subsequently employed for cDNA synthesis and qPCR experiments. Five mRNAs (*LEP, OSBLP10, PRSS23, RNF157* and *SERPINE2*) among the top 5% negative PTc scores and showing at least 2-foldss reduction in their ΔEx values were selected for qPCR profiling. Two reference genes (*TBP* and *ACTB*, as defined by Nygard et al. 2007 [49]) were used for normalization. Accordingly, three of the most DE miRNAs were selected for qPCR profiling (ssc-miR-92b-3p, ssc-miR-148a-3p and ssc-miR-214-3p), plus two non-DE miRNAs for normalization among the most highly expressed in the *lean* vs *obese* small RNA-Seq data set (ssc-let-7a and ssc-miR-23a-3p). Further details about qPCR experimental procedures are available in **Supplementary Methods File S1**. All primers for mRNA and miRNA expression profiling are available at **Table S2.** Raw Cq values for each assay are available at **Table S3**.

3. Results

3.1. The analysis of post-transcriptional regulation in muscle samples from fasting and fed Duroc gilts

Identification of genes predicted to be post-transcriptionally regulated by miRNAs

After the processing, mapping and quantification of mRNA and miRNA expression levels in GM skeletal muscle samples encompassing 11 fasting (*AL-T0*) and 12 fed (*AL-T2*) Duroc gilts, an average of 45.2 million reads per sample (~93%) were successfully mapped to genes annotated in the Sscrofa11.1 v.103 assembly (N = 31,908, including protein coding and non-coding genes). Besides, an average of 2.2 million reads per sample (~42%) mapped to annotated porcine miRNA genes (N = 370).

A total of 30,322 (based on exonic reads) and 22,769 (based on intronic reads) genes were successfully quantified after splitting the reference Sscrofa11.1 v.103 assembly between exonic and intronic ranges. The exonic fraction displayed an average of 1,923.94 estimated counts per gene, whereas the intronic fraction showed an average of 83.02 counts per gene. In other words, exonic counts were ~23 fold more abundant than those corresponding to intronic regions. The fasting group (*AL-T0*) was considered to be the baseline control, i.e., any given upregulation in ΔEx or ΔInt values represents and overexpression in fed (*AL-T2*) Duroc gilts with regard to their fasting (*AL-T0*) counterparts. Finally, PTc scores were obtained from z-scored values of ΔEx – ΔInt estimates and differential expression analyses based on exonic fractions were carried out using the set of 9,492 genes mentioned before.

Differential expression analyses based on exonic fractions identified 454 DE genes (q-value < 0.05). Among those, only genes with |FC| > 2 were retained, making a total of 52 upregulated and 80 downregulated genes (**Table S4, Fig. S2A**). Besides, differential expression analyses on small RNA-seq data for *AL-T0* vs *AL-T2* pigs revealed 16 DE

299 miRNAs (|FC| > 1.5; *q*-value < 0.05), of which 8 were upregulated (representing 6
300 unique miRNA seeds, **Table S5**). The non-redundant seeds of significantly upregulated
301 miRNAs in fed *AL-T2* animals (N = 6; ssc-miR-148a-3p, ssc-miR-7-5p, ssc-miR-30-3p,
302 ssc-miR-151-3p, ssc-miR-374a-3p and ssc-miR-421-5p, **Table S5**) were selected as
303 potential post-transcriptional regulators of GM muscle mRNA expression in response to
304 nutrient supply. EISA results made possible to detect 133 genes with significant effects
305 (|FC| > 2; *q*-value < 0.05, **Table S6**), of which three had > 2-folds reduced ΔEx
306 fractions and two of them had significantly negative PTc scores (*q*-value < 0.05, **Table**
307 **1**).
308 To detect mRNA genes putatively downregulated by miRNAs at the post-transcriptional
309 level, mRNA genes displaying the top 5% negative PTc scores with at least 2-folds ΔEx
310 reduction were selected as putative miRNA-targets (**Fig. S2B**). With this approach, 26
311 mRNA genes were selected (**Table 1**). One of them (ENSSSCG00000049158) did not
312 have a properly annotated 3´-UTR so it was excluded from further analyses. Among this
313 set of 26 genes with high post-transcriptional signals, 18 appeared as significantly
314 downregulated in the differential expression analysis considering their exonic fractions
315 (FC < -2; *q*-value < 0.05, **Table 1** and **Table S4**).
316
317 *Context-based pruning of predicted miRNA-mRNA interactions removes spurious*
318 *unreliable target events*
319 As a first step to determine if genes with highly negative PTc scores and showing a
320 marked reduction in exonic fractions were repressed by upregulated DE miRNAs
321 (**Table S5**), we aimed to investigate the accuracy and reliability of *in silico* predictions
322 regarding miRNA binding sites in their 3'-UTRs (**Table S7**).

We evaluated the presence of enriched binding sites over a random background of expressed genes with no context-based removal of predicted binding sites, applying each one of the three selection criteria reported in Methods independently, as well as by combining them pairwise or altogether. As depicted in **Fig. S3A** and **S3B**, introducing additional context-based filtering criteria for removing spurious unreliable binding site predictions resulted in an overall increased enrichment of miRNA targeted genes within the top 1% (**Fig. S3A**) and 5% (**Fig. S3B**) negative PTc scores and displaying > 2-folds ΔEx reduction. This significantly increased enrichment was more evident when using the AU-rich-based criterion (AU), as shown in **Fig. S3A**). However, we also detected a slight increment when adding the other two context-based removal criteria, i.e., miRNA binding sites located in the middle of the 3'-UTR sequence (M) or located too close (< 15 nts) to the beginning or the end of the 3'-UTR sequences (E). These findings were less evident when taking into consideration the list of the top 5% genes (**Fig. S3B**), probably due to the reduced stringency of gene prioritization and the inclusion of putative false positive candidate genes that are not targeted by the non-redundant seeds of upregulated miRNAs (N = 6, **Table S5**). Nevertheless, an increased enrichment for targeted mRNAs by DE upregulated miRNAs was detectable for all combined filtering criteria, especially for 7mer-A1 binding sites, and probably at the expense of the scarcer and more efficient 8mer binding sites. Based on these results, we decided to apply the three joint criteria (AU, M and E) for enrichment analyses between the set of mRNA genes with high post-transcriptional signals and putatively targeted by miRNAs.

Genes with relevant post-transcriptional signals are enriched for putative miRNA binding sites in their 3'-UTRs

Target prediction and context-based pruning of miRNA-mRNA interactions for mRNA genes displaying the top 5% negative PTc scores and at least 2-folds reductions in the ΔEx exonic fraction (N = 25 after excluding ENSSSCG00000049158) made possible to detect 11 8mer, 21 7mer-m8 and 22 7mer-A1 miRNA binding sites (**Table S7**) corresponding to the non-redundant seeds of DE upregulated miRNAs (N = 6) in *AL-T2* gilts (**Table S5**).

Furthermore, we aimed to determine if mRNA genes showing putative post-transcriptional repression by miRNAs were enriched to be targeted by miRNAs (i.e., assessing whether the number of these genes being putative targets of upregulated miRNAs were significantly higher compared with the whole set of expressed mRNAs). The set of mRNA genes displaying the top 5% (N = 25, **Fig. 1A**) PTc scores and at least 2-folds ΔEx reduction showed a significant (*P*-value < 0.05) enrichment in 8mer, 7mer-m8 and 7mer-A1 sites (**Fig. 1B**), and this was especially relevant when combining these three types of binding sites. More importantly, 21 out of 25 genes displaying the top 5% PTc scores (**Table S7**) were predicted as putative targets of miRNAs upregulated in the GM muscle samples from *AL-T2* fed gilts (**Table 1** and **Table S5**).

We also evaluated the enrichment of the mRNA genes with the top 5% negative PTc scores and at least 2-folds ΔEx reduction (N = 25, **Table 1**) to be targeted by the following sets of miRNAs: (i) Non-redundant downregulated miRNAs in *AL-T2* fed gilts (ssc-miR-1285, ssc-miR-758, ssc-miR-339, sc-miR-22-3p, ssc-miR-296-5p, ssc-miR-129a-3p, ssc-miR-181c and ssc-miR-19b, **Table S5**), (ii) the top 5% most expressed miRNAs, excluding those being upregulated (ssc-miR-1, ssc-miR-133a-3p, ssc-miR-26a, ssc-miR-10b, ssc-miR-378, ssc-miR-99a-5p, ssc-miR-27b-3p, ssc-miR-30d, ssc-miR-486 and ssc-let-7f-5p) and (iii) for an iteration (N = 100) of random sets of 10 expressed miRNAs, irrespective of their DE and abundance status, as a control

test. None of these additional analyses recovered a significant enrichment for any type of the three considered miRNA target subtypes (**Fig. 1B**).

The gene with the highest and significant PTc score was the Dickkopf WNT Signaling Pathway Inhibitor 2 (*DKK2)* locus (**Table 1**), meaning that this gene was the most one with the highest putative miRNA-driven downregulation and no additional transcriptional influence. Moreover, the DKK2 locus was the only gene harboring two miRNA 8mer binding sites (**Table S7**), although it was not among the most highly DE mRNA genes according to differential expression analyses (**Table S4**). As depicted in **Table 1**, only suggestive significant differences in mean expression were found for DKK2 transcripts. Besides, among the set of mRNA genes displaying the top 5% PTc scores and at least 2-folds ΔEx reduction (**Table 1**), 5 were not DE, and 3 of them only showed suggestive DE, while the rest of DE mRNAs displayed a wide range of significance (**Table S4**). The divergence between EISA and differential expression results is also shown in **Fig. 1C**, where not all the mRNA genes highlighted by EISA (**Fig. 1A**) were DE downregulated loci.

The miRNAs with the highest number of significant miRNA-mRNA interactions (in terms of correlations between their expression levels) were ssc-miR-30a-3p and ssc-miR-421-5p, which showed 9 and 8 significant miRNA-mRNA interactions, followed by ssc-miR-148-3p with 4 significant interactions with mRNA genes showing significant post-transcriptional signals (**Table S7**).

Genes showing post-transcriptional regulatory signals predominantly covary at the exonic level

To further elucidate whether genes displaying the top 5% PTc scores are strong candidates to be regulated by miRNAs according to in silico predictions (N = 21), we

evaluated the covariation patterns among them and with the whole set of DE mRNA genes (*q*-value < 0.05, N = 454) by using RNA-seq data from *AL-T0* and *AL-T2* gilts. If multiple genes are downregulated by any upregulated miRNAs in a coordinated manner, we would expect to observe a reduced abundance in their mature spliced mRNA forms but not in the corresponding primary transcripts, i.e., we would detect a covariation only for the exonic fractions (but not for the intronic ones). In other words, the intronic fraction, eventually spliced and degraded in the nucleus, should not reflect any posterior post-transcriptional regulatory effects in the cytoplasm, so little or null covariation might be expected.

By calculating CES values (see Methods) for genes with the top 5% negative PTc scores and 2-folds ΔEx reduction that are putatively targeted by DE upregulated miRNAs (N = 21), we obtained an estimation of the fold change in their observed covariation with respect to other DE mRNAs (N = 435). CEs values were measured for both their exonic and intronic fractions. Our analyses revealed that these genes showed a significantly increased covariation of approximately 2-folds in their exonic fractions when compared to intronic fractions (**Fig. 1D**). When we iteratively analyzed the observed fold change in covariation for random sets of genes (N = 1,000), they displayed CES ≈ 1, indicative of no covariation (**Fig. 1D**). The observed CES distributions of exonic, intronic and control sets were significantly different (*P*-value = 3.663E-06) after running non-parametric tests (**Fig. 1D**), thus supporting that the genes displaying the top 5% PTc scores are probably repressed by DE upregulated by miRNAs.

From the set of 21 mRNA genes with the top 5% negative PTc scores and at least 2-folds ΔEx reduction that are putatively targeted by DE upregulated miRNAs, 19 showed

an overall increased covariation in their exonic fractions compared with their intronic fractions (**Table S8**).

3.2. Studying post-transcriptional signals in adipocytes metabolism using an independent Duroc-Göttingen minipig population

In this section, we will summarize the main findings obtained in the experimental system represented by adipose tissue samples from Duroc-Göttingen minipigs [26,27]. After pre-processing and filtering of sequenced reads from fat samples obtained from 5 lean and 5 obese individuals, we were able to retrieve ~98.1 and ~0.87 million mRNA and small RNA reads per sample, and ~96.5% and ~73.4% of these reads mapped to annotated porcine mRNA and miRNA genes, respectively. Differential expression analyses revealed a total of 299 DE mRNAs (q-value < 0.05), of which 52 mRNAs were downregulated and 95 were upregulated (|FC| > 2; q-value < 0.05), respectively (**Table S9**). Regarding miRNAs, only one gene (ssc-miR-92b-3p) was significantly upregulated in *lean* pigs (|FC| > 2; q-value < 0.05), while 7 additional miRNAs showed suggestive differential expression (P-value < 0.01), of which 4 were downregulated and one of them (ssc-miR-92a) shared the same seed sequence with ssc-miR-92b-3p (**Table S10**).

After running EISA on the mRNA expression profiles for exonic and intronic fractions, a total of 44 downregulated mRNAs in *lean* pigs displayed the top 5% PTc scores with reduced ΔEx > 2-folds (**Table S11, Fig. 2A**). One of them (ENSSSCG00000016928) did not have a properly annotated 3´-UTR so it was excluded from further analyses. The whole set of mRNA genes from EISA results is available at **Table S12**. Among this set of genes with high post-transcriptional signals, 13 appeared as significantly downregulated (FC < -2; q-value < 0.05) and 9 had suggestive repression (P-value < 0.01) in the differential expression analysis considering their exonic fractions (**Table S9**

and **S11**). In this dataset, the sestrin 3 (*SESN3*) locus showed the second highest negative PTc score, but was the only one among the rest of highlighted genes where a significant post-transcriptional signal was observed (**Table S11**), i.e., equivalent to the *DKK2* gene in Duroc pigs, this was the only locus showing post-transcriptional regulation with no additional co-occurring transcriptional signal. Such strong downregulation was also evidenced in differential expression analyses, where it was the most significantly DE gene (**Table S9**).

From these set of genes, 25 out of the 43 mRNA genes analyzed for miRNA binding sites were classified as putative targets of the set of miRNAs upregulated in *lean* pigs (ssc-miR-92b-3p, ssc-miR-148a-3p, ssc-miR-204 and ssc-miR-214-3p; **Table S10**). Target prediction and context-based pruning of miRNA-mRNA interactions for mRNA genes displaying the top 5% negative PTc scores and at least 2-folds reductions in the ΔEx exonic fraction (N = 43, after excluding ENSSSCG00000016928) made possible to detect 8 8mer, 21 7mer-m8 and 24 7mer-A1 miRNA binding sites (**Table S13**) corresponding to the non-redundant seeds of selected upregulated miRNAs (N = 4) in *lean* minipigs (**Table S10**). The *SESN3* gene showed the highest number of predicted putative miRNA target sites in its 3´-UTR (**Table S13**).

Enrichment analyses for the set of putative miRNA target genes with the top 5% negative PTc scores and at least 2-folds ΔEx reduction (N = 25, **Table S11**) revealed no significant enrichment for the three types of miRNA target sites considered, although a slight increase when considering 8mer + 7mer-m8 binding sites and all three types together could be observed (**Fig. 2B**). Among this set of genes (N = 25), 7 appeared as significantly downregulated (FC < -2; *q*-value < 0.05) and 6 had suggestive repression (*P*-value < 0.01) in the differential expression analysis considering their exonic fractions (**Table S9** and **S11**, **Fig. 2C**).

In agreement with results obtained for the *AL-T0* vs *AL-T2* contrast, the exonic fraction of the mRNA genes putatively targeted by upregulated miRNAs in lean pigs (N = 25) showed approximately 2-folds significantly increased covariation (P-value 2.703E-02) with regard to their intronic fraction (**Fig. 2D**). Besides, 18 out of these 25 mRNA genes showed an overall increased covariation in their exonic fractions compared with their intronic fractions, expressed as the increment in their CES values (ΔCES = exonic CES – intronic CES, **Table S14**).

Given the abundance of adipose tissue samples, we used them to carry out qPCR analyses with the aim of validating whether several mRNAs among the top 5% negative PTc scores and with at least 2-folds ΔEx reduction, as well as upregulated miRNAs display patterns of expression consistent with those obtained in RNA-seq and small RNA-seq experiments. To this end, we selected 5 mRNAs (*LEP*, *OSBPL10*, *PRSS23*, *RNF157* and *SERPINE2*) and 3 miRNAs (ssc-miR-148a-30, ssc-miR-214-3p and ssc-miR-92b-3p) for qPCR expression profiling. All the analyzed mRNA genes showed a reduced expression in *lean* pigs compared with their *obese* counterparts (**Fig. 2E**) and the *LEP* gene was the most significantly downregulated gene (log_2FC = -1.953; *P*-value = 1.120E-03), This result was in agreement with the strong downregulation observed in differential expression analyses based on RNA-Seq data ((log_2FC = -1.957; *q*-value = 3.443E-03, **Table S9**). With regard to miRNAs, the opposite pattern of expression was observed, with all the three profiled miRNA genes being upregulated in *lean* pigs. Moreover, as reported in **Table S10**, the ssc-miR-92b-3p gene was the miRNA with the most significant upregulation as evidenced in qPCR analyses (*P*-value = 3.57E-02, **Fig. 2F**).

4. Discussion

The use of EISA for post-transcriptional signals prioritization combined with target prediction of upregulated miRNAs, as well as enrichment analyses on the set of selected targeted genes and their coordinated covariation reinforced the usefulness of this approach to infer functional miRNA-mRNA interactions.

We have observed that the majority of mRNA genes with highly negative PTc scores, i.e., predominantly downregulated at their exonic fractions, also had a coordinated downregulatory effect in their intronic fractions, taken as a proxy of transcriptional repression. This was evidenced by the overall low significance of post-transcriptional signals within the mRNA genes with the top 5% negative PTc scores and reduced ΔEx in both analyzed experimental conditions (**Tables 1** and **S11**). Only two genes (*DKK2* and *NAV2*) in *AL-T0* vs *AL-T2* and one gene (*SESN3*) in the *lean* vs *obese* contrasts showed significant PTc scores (q-value < 0.05, **Table 1** and **S11**), revealing that, overall, a coordinated downregulatory effect at transcriptional and post-transcriptional level was present, which is in agreement with previous reports using EISA [14,15]. However, it is worth noting that we did not consider the significance of PTc scores as a relevant criterion for prioritizing putative post-transcriptionally downregulated genes, as these will appear as significant when the post-transcriptional activity is the only mechanism modulating the target gene expression profile. Only co-occurring yet opposite transcriptional and post-transcriptional events or single post-transcriptional signals would arise as significant, excluding those genes with both coordinated downregulation at the post-transcriptional level.

We decided to use the intronic fraction of expressed mRNAs as a proxy of their transcriptional activity. In this way, the intronic fraction might reflect an approximation to the transcriptional activity of yet unspliced mRNA transcripts leading to the

accumulation of intronic sequences prior to their debranching and degradation by exonucleases. The use of intronic fractions as a proxy of transcription allows the use of RNA-seq datasets to apply EISA without the need of further experimental procedures and it can also be applied to investigate transcriptional regulatory signals [15]. Previous reports have also explored the use of specific techniques to capture nascent mRNA transcripts before they are spliced [50–52], and these have been used to account for the transcriptional activity in a similar approach to EISA [53]. Although more advanced methodologies able to measure transient transcription of mRNAs might provide a better resolution for future experimental designs [53], EISA would be still useful to explore already available RNA-seq data where additional experiments are no longer possible.

Since the efficacy of miRNA targeting depends on the context of the target site within the 3'-UTR [43], we have described the usefulness of introducing context-based filtering criteria for removing spurious *in silico*-predicted target sites for miRNAs. By using enrichment analyses, we were able to link the downregulated mRNAs at their exonic fractions to upregulated miRNAs that were putatively targeting them and triggering their observed decay in differential expression analyses. The influence of other non-DE highly expressed miRNAs or downregulated miRNAs was discarded by the lack of predicted targeted mRNA genes with high post-transcriptional downregulatory signals for such miRNAs. Overall, the increase in enrichment significance shown for targeted mRNAs with post-transcriptional signals and upregulated miRNAs, as opposed to other highly expressed and/or downregulated miRNAs, revealed the ability of context-based filtering criteria to discriminate and remove weak or false positive target sites located within unfavored regions of the 3'-UTR. However, highly efficient target sites such as those of type 8mer, although scarcer than 7mer-m8 sites, might still be functional even at unfavored positions [43,54,55].

546 This may partially explain the relative lack of 8mer sites found in the top post-
547 transcriptionally regulated mRNA genes in both experimental setups.

548 We further hypothesized that genes showing relevant post-transcriptional
549 downregulatory effects might be regulated by the same set of significantly upregulated
550 miRNAs, which could induce shared covariation in their expression profiles at the
551 exonic level. On the contrary, their intronic fractions would be mainly unaffected, as
552 introns would have been excised prior to any given miRNA-driven downregulation, if
553 occurring. In this way, an increased gene covariation might be detectable within the sets
554 of commonly targeted mRNA genes with relevant post-transcriptional signals at the
555 exon but not at the intron level, as opposed to covariation events of these set of genes
556 with the rest of DE genes. Our results indicated an increased degree of the observed
557 covariation between genes with high post-transcriptional signals at their exonic
558 fractions, highlighting a putative coordinated downregulation by the set of significantly
559 upregulated miRNAs.

560 From the analysis of top mRNA genes showing the strongest post-transcriptional
561 downregulatory effects in fasted (*AL-T0*) vs fed (*AL-T2*) gilts, several biological
562 functions putatively regulated by miRNAs were revealed. The *DKK2* gene was the one
563 showing the highest negative PTc score, and its post-transcriptional regulatory signal
564 was also significant (**Table 1**), meaning that no additional coordinated transcriptional
565 downregulation was found for this particular gene. Moreover, this gene also showed the
566 strongest covariation difference in its exonic fraction compared with its intronic fraction
567 (**Table S13**). This consistent post-transcriptional regulatory effect might be explained
568 by the presence of two miRNA target sites of type 8mer in its 3´-UTR for ssc-miR-421-
569 5p and ssc-miR-30a-3p, two highly DE and upregulated miRNAs (**Table S5**). Besides,
570 ssc-miR-30e-3p, a miRNA sharing its seed and regulatory effect with ssc-miR-30a-3p,

was also upregulated in fed (*AL-T2*) gilts, which would reinforce the repression of their targeted mRNA transcripts. The *DKK2* gene is a member of the dickkopf family that inhibits the Wnt signaling pathway through its interaction with the LDL-receptor related protein 6 (*LRP6*). Its repression has been associated with reduced blood-glucose levels and improved glucose uptake [56], as well as with improved adipogenesis [57] and inhibition of aerobic glycolysis [58]. These results would be in agreement with the increased glucose usage and triggered adipogenesis in muscle tissue after nutrient supply. Other additional relevant post-transcriptionally downregulated mRNA genes found by EISA were: (i) pyruvate dehydrogenase kinase 4 (*PDK4*), a mitochondrial enzyme that inhibits pyruvate to acetyl-CoA conversion and hinders glucose utilization promoting fatty acids oxidation in energy-deprived cells under fasting conditions [59,60], (ii) interleukin 18 (*IL18*), involved in controlling energy homeostasis in the muscle by inducing AMP-activated protein kinase (AMPK) [61], a master metabolic regulator that is suppressed upon nutrient influx in cells [62], (iii) nuclear receptor subfamily 4 group A member 3 (*NR4A3*), which activates both glycolytic and glycogenic factors [63], as well as β-oxidation in muscle cells [64], (iv) acetylcholine receptor subunit α (*CHRNA1*) of muscle cells, that is linked to the inhibition of nicotine-dependent *STAT3* upregulation [65] that results in protection against insulin resistance in muscle [66], (v) PBX homeobox 1 (*PBX1*), a regulator of adipocyte differentiation [67], (vi) Tet methylcytosine dioxygenase 2 (*TET2*), linked to glucose-dependent AMPK phosphorylation [68] and (vii) BTB domain and CNC homolog (*BACH2*), associated with mTOR complex 2 (mTORC2) glucose-dependent activation [69,70] and the repression of forkhead box protein O1 (*FOXO1*) [71] and *PDK4* in a coordinated manner [7,72]. Overall, the highlighted downregulated genes in the muscle of fed gilts

after nutrient supply pointed towards a common regulatory function of miRNAs in modulating glucose uptake and energy homeostasis of the skeletal myocytes.

Although miRNAs were the major post-transcriptional regulators that we considered in this study, it is important to remark that other additional post-transcriptional modifications and interactions might be responsible of the observed downregulation of mRNAs [73–77]. This could explain the presence of non-miRNA targets within the top post-transcriptional signals, as well as additional regulatory mechanisms not directly involved in energy homeostasis or glucose usage among the highlighted genes. For instance, three circadian clock-related mRNA genes that showed high post-transcriptional signals were the circadian associated repressor of transcription (*CIART*), period 1 (*PER1*) and salt inducible kinase 1 (*SIK1*), yet the first two were not detected as targets of differentially expressed miRNAs, as shown in **Table 1**. As previously reported for this experimental design [22], the presence of several genes showing abundance differences might reflect a tight feedback interplay among them, where their expression and accumulation are coordinately regulated.

Regarding EISA results in RNA-seq profiles of adipocytes from lean and obese Duroc-Göttingen minipigs, several of the mRNA genes that showed high post-transcriptional repression were tightly involved in the regulation of lipids metabolism and energy homeostasis. The gene showing the highest post-transcriptional signal was the estrogen related receptor γ (*ESRRG*), which modulates oxidative metabolism and mitochondrial function in adipose tissue and that results in the downregulation of adipocyte differentiation when repressed [78]. The second locus highlighted by EISA was sestrin 3 (*SESN3*), an activator of mTORC2 and PI3K/AKT signaling pathway [79] that protects against insulin resistance and promotes lipolysis when inhibited [80]. This gene showed the most significant downregulation in lean pigs (**Table S9**), and gathered

multiple putative binding sites for all the four upregulated miRNAs analyzed (**Table S10** and **S13**). The sterile α motif domain containing 4A (*SAMD4A*) knockdown has been linked to the inhibition of preadipocyte differentiation and leanness phenotype [81,82]. The prostaglandin F2- receptor protein (PTGFR) overexpression has been associated with hypertension and obesity risk [83], and its repression improved insulin sensitivity and glucose homeostasis [84]. High expression of serpin E1 and E2 (*SERPINE1*, *SERPINE2*) were linked to obesogenic states and diabetic symptoms [85], while their inhibition improved glucose metabolism [86]. The serine protease 23 (PRSS23) regulates insulin sensitivity and cytokine expression in adipose tissue, and its downregulation confers protective effects against inflammation and reduced fasting glucose level improving insulin resistance [87]. A high expression of ring finger protein 157 (*RNF157*) has been described in adipose tissue with high fatness profiles and increased autophagy [88]. Silencing of ORP10 protein, encoded by the *OSBLP10* gene, promotes low-density lipoprotein (LDL) synthesis and inhibits lipogenesis [89]. The serum levels of glycosylphosphatidylinositol phospholipase 1 (GPLD1) are regulated by insulin and glucose metabolism [90] and linked to the development of insulin resistance and metabolic syndrome [91]. Overexpression of neutrophil cytosolic 2 (*NCF2*), the gene showing the highest increase in covariation at the exonic fraction (**Table S14**), was described in obese humans [92]. The repression of RAP1 GTPase activating protein (RAP1GAP) promotes RAP1 activity, which protects against obesity and insulin and glucose resistance [93,94]. Finally, leptin production was also decreased in lean pigs (**Table S10**). This key adipokine is mainly produced in adipose tissue [95] and regulates appetite, energy expenditure and body weight [96,97].

In summary, similar to what we found for glucose metabolism and energy homeostasis in fasted vs fed Duroc pigs, we were also able to describe a set of post-transcriptionally

645 downregulated genes in lean minipigs tightly related to adipose tissue metabolism
646 regulation compatible with explaining, at least partially, the differences in their fatness
647 profile compared to their obese counterparts.
648
649

650 # 5. Conclusions

651 In this study we have implemented an exon/intron split analysis of RNA-seq data from
652 skeletal muscle and adipose tissue of pigs, in order to disentangle miRNA-driven post-
653 transcriptional signals that are not evident from the analysis of differentially expressed
654 mRNAs. In this way, we were able to prioritize regulatory relationships between
655 upregulated miRNAs and their putative mRNA targets. We demonstrated that
656 incorporating context-based pruning of *in silico*-predicted miRNA targets increased the
657 reliability of the putative miRNA-mRNA interactions. Besides, these downregulated
658 mRNAs with relevant post-transcriptional signals were significantly enriched for being
659 cooperatively targeted by a set of upregulated miRNAs, as opposed to other highly
660 expressed and/or downregulated miRNAs. The majority of these genes showed an
661 average of 2-folds increase in expression covariation in their exonic fractions compared
662 to their intronic fractions, a result that reinforced their putative post-transcriptional
663 downregulation by miRNA-driven transcript degradation. Our results highlighted an
664 efficient framework to prioritize mRNA genes showing post-transcriptional signals
665 linked to miRNA-driven downregulation using exonic and intronic fractions of
666 commonly available RNA-seq datasets.

667
668

Support

The present research work was funded by grants AGL2013-48742-C2-1-R and AGL2013-48742-C2-2-R awarded by the Spanish Ministry of Economy and Competitivity. E. Mármol-Sánchez was funded with a PhD fellowship FPU15/01733 awarded by the Spanish Ministry of Education and Culture (MECD). YRC is recipient of a Ramon y Cajal fellowship (RYC2019-027244-I) from the Spanish Ministry of Science and Innovation.

Conflict of interest

The authors declare no conflict of interest.

Acknowledgements

The authors would like to thank the Department of Veterinary Animal Sciences in the Faculty of Health and Medical Sciences of the University of Copenhagen for providing sequencing data and their facilities and resources for qPCR experiments. We also acknowledge Selección Batallé S.A. for providing animal material and the support of the Spanish Ministry of Economy and Competitivity for the Center of Excellence Severo Ochoa 2020–2023 (CEX2019-000902-S) grant awarded to the Centre for Research in Agricultural Genomics (CRAG, Bellaterra, Spain). Thanks also to the CERCA Programme of the Generalitat the Catalunya for their support.

References

[1] N.J. Martinez, A.J.M. Walhout, The interplay between transcription factors and microRNAs in genome-scale regulatory networks, BioEssays. 31 (2009) 435–445. doi:10.1002/bies.200800212.

[2] D.P. Bartel, Metazoan microRNAs, Cell. 173 (2018) 20–51. doi:10.1016/j.cell.2018.03.006.

[3] C.M.J. Mentzel, C. Anthon, M.J. Jacobsen, P. Karlskov-Mortensen, C.S. Bruun, C.B. Jørgensen, J. Gorodkin, S. Cirera, M. Fredholm, Gender and obesity specific microRNA expression in adipose tissue from lean and obese pigs., PLoS One. 10 (2015) e0131650. doi:10.1371/journal.pone.0131650.

[4] H. Han, S. Gu, W. Chu, W. Sun, W. Wei, X. Dang, Y. Tian, K. Liu, J. Chen, miR-17-5p regulates differential expression of *NCOA3* in pig intramuscular and subcutaneous adipose tissue, Lipids. 52 (2017) 939–949. doi:10.1007/s11745-017-4288-4.

[5] W. Wei, B. Li, K. Liu, A. Jiang, C. Dong, C. Jia, J. Chen, H. Liu, W. Wu, Identification of key microRNAs affecting drip loss in porcine longissimus dorsi by RNA-Seq, Gene. 647 (2018) 276–282. doi:10.1016/j.gene.2018.01.005.

[6] S. Xie, X. Li, L. Qian, C. Cai, G. Xiao, S. Jiang, B. Li, T. Gao, W. Cui, L.L. Guan, An integrated analysis of mRNA and miRNA in skeletal muscle from myostatin-edited Meishan pigs, Genome. 62 (2019) 305–315. doi:10.1139/gen-2018-0110.

[7] E. Mármol-Sánchez, Y. Ramayo-Caldas, R. Quintanilla, T.F. Cardoso, R. González-Prendes, J. Tibau, M. Amills, Co-expression network analysis predicts a key role of microRNAs in the adaptation of the porcine skeletal muscle to nutrient supply, J. Anim. Sci. Biotechnol. 11 (2020) 10. doi:10.1186/s40104-019-

719 0412-z.

720 [8] M.A. Iqbal, A. Ali, F. Hadlich, M. Oster, H. Reyer, N. Trakooljul, V.
721 Sommerfeld, M. Rodehutscord, K. Wimmers, S. Ponsuksili, Dietary phosphorus
722 and calcium in feed affects miRNA profiles and their mRNA targets in jejunum
723 of two strains of laying hens, Sci. Rep. 11 (2021) 13534. doi:10.1038/S41598-
724 021-92932-3.

725 [9] A. Ali, E. Murani, F. Hadlich, X. Liu, K. Wimmers, S. Ponsuksili, In utero fetal
726 weight in pigs is regulated by microRNAs and their target genes, Genes. 12
727 (2021) 1264. doi:10.3390/genes12081264.

728 [10] D. Gaidatzis, L. Burger, M. Florescu, M.B. Stadler, Analysis of intronic and
729 exonic reads in RNA-seq data characterizes transcriptional and post-
730 transcriptional regulation, Nat. Biotechnol. 33 (2015) 722–729.
731 doi:10.1038/nbt.3269.

732 [11] A. Ameur, A. Zaghlool, J. Halvardson, A. Wetterbom, U. Gyllensten, L.
733 Cavelier, L. Feuk, Total RNA sequencing reveals nascent transcription and
734 widespread co-transcriptional splicing in the human brain., Nat. Struct. Mol.
735 Biol. 18 (2011) 1435–40. doi:10.1038/nsmb.2143.

736 [12] J.M. Gray, D.A. Harmin, S.A. Boswell, N. Cloonan, T.E. Mullen, J.J. Ling, N.
737 Miller, S. Kuersten, Y.-C. Ma, S.A. McCarroll, S.M. Grimmond, M. Springer,
738 SnapShot-Seq: a method for extracting genome-wide, in vivo mRNA dynamics
739 from a single total RNA sample., PLoS One. 9 (2014) e89673.
740 doi:10.1371/journal.pone.0089673.

741 [13] G.-J. Hendriks, D. Gaidatzis, F. Aeschimann, H. Großhans, Extensive oscillatory
742 gene expression during C. elegans larval development., Mol. Cell. 53 (2014)
743 380–92. doi:10.1016/j.molcel.2013.12.013.

[14] J. Cursons, K.A. Pillman, K.G. Scheer, P.A. Gregory, M. Foroutan, S. Hediyeh-Zadeh, J. Toubia, E.J. Crampin, G.J. Goodall, C.P. Bracken, M.J. Davis, Combinatorial targeting by microRNAs co-ordinates post-transcriptional control of EMT, Cell Syst. 7 (2018) 77-91.e7. doi:10.1016/j.cels.2018.05.019.

[15] K.A. Pillman, K.G. Scheer, E. Hackett-Jones, K. Saunders, A.G. Bert, J. Toubia, H.J. Whitfield, S. Sapkota, L. Sourdin, H. Pham, T.D. Le, J. Cursons, M.J. Davis, P.A. Gregory, G.J. Goodall, C.P. Bracken, Extensive transcriptional responses are co-ordinated by microRNAs as revealed by Exon–Intron Split Analysis (EISA), Nucleic Acids Res. 47 (2019) 8606-8619. doi:10.1093/nar/gkz664.

[16] D. Pérez-Montarelo, A. Fernández, C. Barragán, J.L. Noguera, J.M. Folch, M.C. Rodríguez, C. Óvilo, L. Silió, A.I. Fernández, Transcriptional characterization of porcine leptin and leptin receptor genes, PLoS One. 8 (2013) e66398. doi:10.1371/journal.pone.0066398.

[17] C. Ovilo, R. Benítez, A. Fernández, Y. Núñez, M. Ayuso, A.I. Fernández, C. Rodríguez, B. Isabel, A.I. Rey, C. López-Bote, L. Silió, Longissimus dorsi transcriptome analysis of purebred and crossbred Iberian pigs differing in muscle characteristics., BMC Genomics. 15 (2014) 413. doi:10.1186/1471-2164-15-413.

[18] A. Puig-Oliveras, Y. Ramayo-Caldas, J. Corominas, J. Estellé, D. Pérez-Montarelo, N.J. Hudson, J. Casellas, J.M. Folch, M. Ballester, Differences in muscle transcriptome among pigs phenotypically extreme for fatty acid composition., PLoS One. 9 (2014) e99720. doi:10.1371/journal.pone.0099720.

[19] C.M. Pilcher, C.K. Jones, M. Schroyen, A.J. Severin, J.F. Patience, C.K. Tuggle, J.E. Koltes, Transcript profiles in longissimus dorsi muscle and subcutaneous adipose tissue: A comparison of pigs with different postweaning growth rates, J.

769 Anim. Sci. 93 (2015) 2134–2143. doi:10.2527/jas.2014-8593.

770 [20] M. Ayuso, A. Fernández, Y. Núñez, R. Benítez, B. Isabel, A.I. Fernández, A.I.
771 Rey, A. González-Bulnes, J.F. Medrano, Á. Cánovas, C.J. López-Bote, C. Óvilo,
772 Developmental stage, muscle and genetic type modify muscle transcriptome in
773 pigs: Effects on gene expression and regulatory factors involved in growth and
774 metabolism, PLoS One. 11 (2016) e0167858. doi:10.1371/journal.pone.0167858.

775 [21] T.F. Cardoso, A. Cánovas, O. Canela-Xandri, R. González-Prendes, M. Amills,
776 R. Quintanilla, RNA-seq based detection of differentially expressed genes in the
777 skeletal muscle of Duroc pigs with distinct lipid profiles, Sci. Rep. 7 (2017)
778 40005. doi:10.1038/srep40005.

779 [22] T.F. Cardoso, R. Quintanilla, J. Tibau, M. Gil, E. Mármol-Sánchez, O. González-
780 Rodríguez, R. González-Prendes, M. Amills, Nutrient supply affects the mRNA
781 expression profile of the porcine skeletal muscle, BMC Genomics. 18 (2017)
782 603. doi:10.1186/s12864-017-3986-x.

783 [23] J. Horodyska, K. Wimmers, H. Reyer, N. Trakooljul, A.M. Mullen, P.G. Lawlor,
784 R.M. Hamill, RNA-seq of muscle from pigs divergent in feed efficiency and
785 product quality identifies differences in immune response, growth, and
786 macronutrient and connective tissue metabolism, BMC Genomics. 19 (2018)
787 791. doi:10.1186/s12864-018-5175-y.

788 [24] R. Benítez, N. Trakooljul, Y. Núñez, B. Isabel, E. Murani, E. De Mercado, E.
789 Gómez-Izquierdo, J. García-Casco, C. López-Bote, K. Wimmers, C. Óvilo,
790 Breed, diet, and interaction effects on adipose tissue transcriptome in iberian and
791 duroc pigs fed different energy sources, Genes. 10 (2019) 589.
792 doi:10.3390/genes10080589.

793 [25] M. Ballester, M. Amills, O. González-Rodríguez, T.F. Cardoso, M. Pascual, R.

González-Prendes, N. Panella-Riera, I. Díaz, J. Tibau, R. Quintanilla, Role of AMPK signalling pathway during compensatory growth in pigs, BMC Genomics. 19 (2018) 682. doi:10.1186/s12864-018-5071-5.

[26] L.J.A. Kogelman, H.N. Kadarmideen, T. Mark, P. Karlskov-Mortensen, C.S. Bruun, S. Cirera, M.J. Jacobsen, C.B. Jørgensen, M. Fredholm, An F2 pig resource population as a model for genetic studies of obesity and obesity-related diseases in humans: Design and genetic parameters, Front. Genet. 4 (2013) 29. doi:10.3389/fgene.2013.00029.

[27] S.D. Pant, P. Karlskov-Mortensen, M.J. Jacobsen, S. Cirera, L.J.A. Kogelman, C.S. Bruun, T. Mark, C.B. Jørgensen, N. Grarup, E.V.R. Appel, E.A.A. Galjatovic, T. Hansen, O. Pedersen, M. Guerin, T. Huby, P. Lesnik, T.H.E. Meuwissen, H.N. Kadarmideen, M. Fredholm, Comparative analyses of QTLs influencing obesity and metabolic phenotypes in pigs and humans, PLoS One. 10 (2015) e0137356. doi:10.1371/journal.pone.0137356.

[28] M.J. Jacobsen, J.H. Havgaard, C. Anthon, C.M.J. Mentzel, S. Cirera, P.M. Krogh, S. Pundhir, P. Karlskov-Mortensen, C.S. Bruun, P. Lesnik, M. Guerin, J. Gorodkin, C.B. Jørgensen, M. Fredholm, R. Barrès, Epigenetic and transcriptomic characterization of pure adipocyte fractions from obese pigs identifies candidate pathways controlling metabolism, Front. Genet. 10 (2019) 1268. doi:10.3389/fgene.2019.01268.

[29] P. Decaunes, D. Estève, A. Zakaroff-Girard, C. Sengenès, J. Galitzky, A. Bouloumié, Adipose-derived stromal cells: cytokine expression and immune cell contaminants., Methods Mol. Biol. 702 (2011) 151–161. doi:10.1007/978-1-61737-960-4_12.

[30] S. Cirera, Highly efficient method for isolation of total RNA from adipose

819 tissue., BMC Res. Notes. 6 (2013) 472. doi:10.1186/1756-0500-6-472.

820 [31] M. Martin, Cutadapt removes adapter sequences from high-throughput
821 sequencing reads, EMBnet.Journal. 17 (2011) 10. doi:10.14806/ej.17.1.200.

822 [32] A. Warr, N. Affara, B. Aken, H. Beiki, D.M. Bickhart, K. Billis, W. Chow, L.
823 Eory, H.A. Finlayson, P. Flicek, C.G. Girón, D.K. Griffin, R. Hall, G. Hannum,
824 T. Hourlier, K. Howe, D.A. Hume, O. Izuogu, K. Kim, S. Koren, H. Liu, N.
825 Manchanda, F.J. Martin, D.J. Nonneman, R.E. O'Connor, A.M. Phillippy, G.A.
826 Rohrer, B.D. Rosen, L.A. Rund, C.A. Sargent, L.B. Schook, S.G. Schroeder, A.S.
827 Schwartz, B.M. Skinner, R. Talbot, E. Tseng, C.K. Tuggle, M. Watson, T.P.L.
828 Smith, A.L. Archibald, An improved pig reference genome sequence to enable
829 pig genetics and genomics research, Gigascience. 9 (2020) 1–14.
830 doi:10.1093/gigascience/giaa051.

831 [33] D. Kim, B. Langmead, S.L. Salzberg, HISAT: a fast spliced aligner with low
832 memory requirements, Nat. Methods. 12 (2015) 357–360.
833 doi:10.1038/nmeth.3317.

834 [34] B. Langmead, C. Trapnell, M. Pop, S.L. Salzberg, Ultrafast and memory-efficient
835 alignment of short DNA sequences to the human genome, Genome Biol. 10
836 (2009) R25. doi:10.1186/gb-2009-10-3-r25.

837 [35] M. Lawrence, W. Huber, H. Pagès, P. Aboyoun, M. Carlson, R. Gentleman, M.T.
838 Morgan, V.J. Carey, Software for computing and annotating genomic ranges,
839 PLoS Comput. Biol. 9 (2013) e1003118. doi:10.1371/journal.pcbi.1003118.

840 [36] Y. Liao, G.K. Smyth, W. Shi, The R package Rsubread is easier, faster, cheaper
841 and better for alignment and quantification of RNA sequencing reads, Nucleic
842 Acids Res. 47 (2019) e47–e47. doi:10.1093/nar/gkz114.

843 [37] Y. Liao, G.K. Smyth, W. Shi, featureCounts: an efficient general purpose

844 program for assigning sequence reads to genomic features, Bioinformatics. 30
845 (2014) 923–930. doi:10.1093/bioinformatics/btt656.
846 [38] M.D. Robinson, D.J. McCarthy, G.K. Smyth, edgeR: a Bioconductor package for
847 differential expression analysis of digital gene expression data., Bioinformatics.
848 26 (2010) 139–40. doi:10.1093/bioinformatics/btp616.
849 [39] M.D. Robinson, A. Oshlack, A scaling normalization method for differential
850 expression analysis of RNA-seq data, Genome Biol. 11 (2010) R25.
851 doi:10.1186/gb-2010-11-3-r25.
852 [40] Y. Benjamini, Y. Hochberg, Controlling the false discovery rate: a practical and
853 powerful approach to multiple testing, J. R. Stat. Soc. Ser. B. 57 (1995) 289–300.
854 doi:10.2307/2346101.
855 [41] A. Kozomara, M. Birgaoanu, S. Griffiths-Jones, MiRBase: From microRNA
856 sequences to function, Nucleic Acids Res. 47 (2019) D155–D162.
857 doi:10.1093/nar/gky1141.
858 [42] A. Marco, SeedVicious: Analysis of microRNA target and near-target sites, PLoS
859 One. 13 (2018) e0195532. doi:10.1371/journal.pone.0195532.
860 [43] A. Grimson, K.K.H. Farh, W.K. Johnston, P. Garrett-Engele, L.P. Lim, D.P.
861 Bartel, MicroRNA targeting specificity in mammals: determinants beyond seed
862 pairing, Mol. Cell. 27 (2007) 91–105. doi:10.1016/j.molcel.2007.06.017.
863 [44] R.C. Friedman, K.K.H. Farh, C.B. Burge, D.P. Bartel, Most mammalian mRNAs
864 are conserved targets of microRNAs, Genome Res. 19 (2009) 92–105.
865 doi:10.1101/gr.082701.108.
866 [45] A. Reverter, E.K.F. Chan, Combining partial correlation and an information
867 theory approach to the reversed engineering of gene co-expression networks,
868 Bioinformatics. 24 (2008) 2491–2497. doi:10.1093/bioinformatics/btn482.

869 [46] N.S. Watson-Haigh, H.N. Kadarmideen, A. Reverter, PCIT: an R package for
870 weighted gene co-expression networks based on partial correlation and
871 information theory approaches, Bioinformatics. 26 (2010) 411–413.
872 doi:10.1093/bioinformatics/btp674.
873 [47] M. Tarbier, S.D. Mackowiak, J. Frade, S. Catuara-Solarz, I. Biryukova, E. Gelali,
874 D.B. Menéndez, L. Zapata, S. Ossowski, M. Bienko, C.J. Gallant, M.R.
875 Friedländer, Nuclear gene proximity and protein interactions shape transcript
876 covariations in mammalian single cells, Nat. Commun. 11 (2020) 5445.
877 doi:10.1038/s41467-020-19011-5.
878 [48] H.B. Mann, D.R. Whitney, On a test of whether one of two random variables is
879 stochastically larger than the other, Ann. Math. Stat. 18 (1947) 50–60.
880 doi:10.1214/aoms/1177730491.
881 [49] A.B. Nygard, C.B. Jørgensen, S. Cirera, M. Fredholm, Selection of reference
882 genes for gene expression studies in pig tissues using SYBR green qPCR, BMC
883 Mol. Biol. 8 (2007) 67. doi:10.1186/1471-2199-8-67.
884 [50] L.J. Core, J.J. Waterfall, J.T. Lis, Nascent RNA sequencing reveals widespread
885 pausing and divergent initiation at human promoters, Science. 322 (2008) 1845–
886 1848. doi:10.1126/science.1162228.
887 [51] D.B. Mahat, H. Kwak, G.T. Booth, I.H. Jonkers, C.G. Danko, R.K. Patel, C.T.
888 Waters, K. Munson, L.J. Core, J.T. Lis, Base-pair resolution genome-wide
889 mapping of active RNA polymerasesusing precision nuclear run-on (PRO-seq),
890 Nat. Protoc. 11 (2016) 1455. doi:10.1038/nprot.2016.086.
891 [52] A. Blumberg, Y. Zhao, Y.-F. Huang, N. Dukler, E.J. Rice, A.G. Chivu, K.
892 Krumholz, C.G. Danko, A. Siepel, Characterizing RNA stability genome-wide
893 through combined analysis of PRO-seq and RNA-seq data, BMC Biol. 19 (2021)

30. doi:10.1186/s12915-021-00949-x.

[53] R.K. Patel, J.D. West, Y. Jiang, E.A. Fogarty, A. Grimson, Robust partitioning of microRNA targets from downstream regulatory changes, Nucleic Acids Res. 48 (2020) 9724–9746. doi:10.1093/nar/gkaa687.

[54] R. Denzler, S.E. McGeary, A.C. Title, V. Agarwal, D.P. Bartel, M. Stoffel, Impact of microRNA levels, target-site complementarity, and cooperativity on competing endogenous RNA-regulated gene expression, Mol. Cell. 64 (2016) 565-579. doi:10.1016/j.molcel.2016.09.027.

[55] S.E. McGeary, K.S. Lin, C.Y. Shi, T.M. Pham, N. Bisaria, G.M. Kelley, D.P. Bartel, The biochemical basis of microRNA targeting efficacy, Science. 366 (2019) eaav1741. doi:10.1126/science.aav1741.

[56] X. Li, J. Shan, W. Chang, I. Kim, J. Bao, H.-J. Lee, X. Zhang, V.T. Samuel, G.I. Shulman, D. Liu, J.J. Zheng, D. Wu, Chemical and genetic evidence for the involvement of Wnt antagonist Dickkopf2 in regulation of glucose metabolism, Proc. Natl. Acad. Sci. 109 (2012) 11402–11407. doi:10.1073/pnas.1205015109.

[57] J. Yang, B. yin Shi, Dickkopf (Dkk)-2 is a beige fat-enriched adipokine to regulate adipogenesis, Biochem. Biophys. Res. Commun. 548 (2021) 211–216. doi:10.1016/j.bbrc.2021.02.068.

[58] F. Deng, R. Zhou, C. Lin, S. Yang, H. Wang, W. Li, K. Zheng, W. Lin, X. Li, X. Yao, M. Pan, L. Zhao, Tumor-secreted dickkopf2 accelerates aerobic glycolysis and promotes angiogenesis in colorectal cancer, Theranostics. 9 (2019) 1001-1014. doi:10.7150/thno.30056.

[59] J.Y. Jeong, N.H. Jeoung, K.-G. Park, I.-K. Lee, Transcriptional regulation of pyruvate dehydrogenase kinase, Diabetes Metab. J. 36 (2012) 328–35. doi:10.4093/dmj.2012.36.5.328.

[60] S. Zhang, M.W. Hulver, R.P. McMillan, M.A. Cline, E.R. Gilbert, The pivotal role of pyruvate dehydrogenase kinases in metabolic flexibility, Nutr. Metab. 11 (2014) 10. doi:10.1186/1743-7075-11-10.

[61] B. Lindegaard, V.B. Mathews, C. Brandt, P. Hojman, T.L. Allen, E. Estevez, M.J. Watt, C.R. Bruce, O.H. Mortensen, S. Syberg, C. Rudnika, J. Abildgaard, H. Pilegaard, J. Hidalgo, S. Ditlevsen, T.J. Alsted, A.N. Madsen, B.K. Pedersen, M.A. Febbraio, Interleukin-18 activates skeletal muscle AMPK and reduces weight gain and insulin resistance in mice, Diabetes. 62 (2013) 3064–3074. doi:10.2337/DB12-1095.

[62] P. Jiang, L. Ren, L. Zhi, Z. Yu, F. Lv, F. Xu, W. Peng, X. Bai, K. Cheng, L, Quang, X. Zhang, X. Wang, Y. Zhang, D. Yang, X. Hu, R.P. Xiao, Negative regulation of AMPK signaling by high glucose via E3 ubiquitin ligase MG53, Mol. Cell. 81 (2021) 629-637.e5. doi:10.1016/j.molcel.2020.12.008.

[63] C. Zhang, B. Zhang, X. Zhang, G. Sun, X. Sun, Targeting orphan nuclear receptors NR4As for energy homeostasis and diabetes, Front. Pharmacol. 11 (2020) 587457. doi:10.3389/fphar.2020.587457.

[64] M.A. Pearen, J.M. Goode, R.L. Fitzsimmons, N.A. Eriksson, G.P. Thomas, G.J. Cowin, S.C. Wang, Z.K. Tuong, G.E. Muscat, Transgenic muscle-specific Nor-1 expression regulates multiple pathways that effect adiposity, metabolism, and endurance, Mol. Endocrinol. 27 (2013) 1897–1917. doi:10.1210/me.2013-1205.

[65] S. Xu, H. Ni, H. Chen, Q. Dai, The interaction between STAT3 and nAChRα1 interferes with nicotine-induced atherosclerosis via Akt/mTOR signaling cascade, Aging. 11 (2019) 8120–8138. doi:10.18632/aging.102296.

[66] L. Zhang, Z. Chen, Y. Wang, D.J. Tweardy, W.E. Mitch, Stat3 activation induces insulin resistance via a muscle-specific E3 ubiquitin ligase Fbxo40, Am. J.

944 Physiol. Endocrinol. Metab. 318 (2020) E625–E635.
945 doi:10.1152/ajpendo.00480.2019.
946 [67] M.C. Monteiro, M. Sanyal, M.L. Cleary, C. Sengenès, A. Bouloumié, C. Dani, N.
947 Billon, PBX1: a novel stage-specific regulator of adipocyte development, Stem
948 Cells. 29 (2011) 1837–1848. doi:10.1002/stem.737.
949 [68] D. Wu, D. Hu, H. Chen, G. Shi, I.S. Fetahu, F. Wu, K. Rabidou, R. Fang, L. Tan,
950 S. Xu, H. Liu, C. Argueta, L. Zhang, F. Mao, G. Yan, J. Chen, Z. Dong, R. Lv,
951 Y. Xu, M. Wang, Y. Ye, S. Zhang, D. Duquette, S. Geng, C. Yin, C.G. Lian, G.F.
952 Murphy, G.K. Adler, R. Garg, L. Lynch, P. Yang, Y. Li, F. Lan, J. Fan, Y. Shi,
953 Y.G. Shi, Glucose-regulated phosphorylation of TET2 by AMPK reveals a
954 pathway linking diabetes to cancer, Nature. 559 (2018) 637–641.
955 doi:10.1038/s41586-018-0350-5.
956 [69] T. Tamahara, K. Ochiai, A. Muto, Y. Kato, N. Sax, M. Matsumoto, T. Koseki, K.
957 Igarashi, The mTOR-Bach2 cascade controls cell cycle and class switch
958 recombination during B cell differentiation, Mol. Cell. Biol. 37 (2017) e00418-
959 17. doi:10.1128/mcb.00418-17.
960 [70] G. Leprivier, B. Rotblat, How does mTOR sense glucose starvation? AMPK is
961 the usual suspect, Cell Death Discov. 6 (2020) 27. doi:10.1038/S41420-020-
962 0260-9.
963 [71] A. Itoh-Nakadai, M. Matsumoto, H. Kato, J. Sasaki, Y. Uehara, Y. Sato, R.
964 Ebina-Shibuya, M. Morooka, R. Funayama, K. Nakayama, K. Ochiai, A. Muto,
965 K. Igarashi, A Bach2-Cebp gene regulatory network for the commitment of
966 multipotent hematopoietic progenitors, Cell Rep. 18 (2017) 2401–2414.
967 doi:10.1016/j.celrep.2017.02.029.
968 [72] K. Gopal, B. Saleme, R. Al Batran, H. Aburasayn, A. Eshreif, K.L. Ho, W.K.

969 Ma, M. Almutairi, F. Eaton, M. Gandhi, E.A. Park, G. Sutendra, J.R. Ussher,
970 FoxO1 regulates myocardial glucose oxidation rates via transcriptional control of
971 pyruvate dehydrogenase kinase 4 expression, Am. J. Physiol. Circ. Physiol. 313
972 (2017) H479–H490. doi:10.1152/ajpheart.00191.2017.
973 [73] T. Glisovic, J.L. Bachorik, J. Yong, G. Dreyfuss, RNA-binding proteins and
974 post-transcriptional gene regulation, FEBS Lett. 582 (2008) 1977–1986.
975 doi:10.1016/j.febslet.2008.03.004.
976 [74] B.S. Zhao, I.A. Roundtree, C. He, Post-transcriptional gene regulation by mRNA
977 modifications, Nat. Rev. Mol. Cell Biol. 18 (2017) 31.
978 doi:10.1038/nrm.2016.132.
979 [75] M.W. Hentze, A. Castello, T. Schwarzl, T. Preiss, A brave new world of RNA-
980 binding proteins, Nat. Rev. Mol. Cell Biol. 19 (2018) 327–341.
981 doi:10.1038/nrm.2017.130.
982 [76] Q. Sun, Q. Hao, K. V. Prasanth, Nuclear long noncoding RNAs: key regulators
983 of gene expression, Trends Genet. 34 (2018) 142–157.
984 doi:10.1016/j.tig.2017.11.005.
985 [77] A. Velázquez-Cruz, B. Baños-Jaime, A. Díaz-Quintana, M.A.D. la Rosa, I. Díaz-
986 Moreno, Post-translational control of RNA-binding proteins and disease-related
987 dysregulation, Front. Mol. Biosci. 8 (2021) 658852.
988 doi:10.3389/fmolb.2021.658852.
989 [78] M. Kubo, N. Ijichi, K. Ikeda, K. Horie-Inoue, S. Takeda, S. Inoue, Modulation of
990 adipogenesis-related gene expression by estrogen-related receptor γ during
991 adipocytic differentiation, Biochim. Biophys. Acta - Gene Regul. Mech. 1789
992 (2009) 71–77. doi:10.1016/j.bbgram.2008.08.012.
993 [79] X. Huang, G. Liu, J. Guo, Z. Su, The PI3K/AKT pathway in obesity and type 2

diabetes, Int. J. Biol. Sci. 14 (2018) 1483. doi:10.7150/ijbs.27173.

[80] R. Tao, X. Xiong, S. Liangpunsakul, X.C. Dong, Sestrin 3 protein enhances hepatic insulin sensitivity by direct activation of the mTORC2-Akt signaling, Diabetes. 64 (2015) 1211–1223. doi:10.2337/db14-0539.

[81] Z. Chen, W. Holland, J.M. Shelton, A. Ali, X. Zhan, S. Won, W. Tomisato, C. Liu, X. Li, E.M.Y. Moresco, B. Beutler, Mutation of mouse *Samd4* causes leanness, myopathy, uncoupled mitochondrial respiration, and dysregulated mTORC1 signaling, Proc. Natl. Acad. Sci. 111 (2014) 7367–7372. doi:10.1073/pnas.1406511111.

[82] Y. Liu, H. Liu, Y. Li, R. Mao, H. Yang, Y. Zhang, Y. Zhang, P. Guo, D. Zhan, T. Zhang, Circular RNA *SAMD4A* controls adipogenesis in obesity through the miR-138-5p/EZH2 axis, Theranostics. 10 (2020) 4705–4719. doi:10.7150/thno.42417.

[83] B. Xiao, S.M. Gu, M.J. Li, J. Li, B. Tao, Y. Wang, Y. Wang, S. Zuo, Y. Shen, Y. Yu, D. Chen, G. Chen, D. Kong, J. Tang, Q. Liu, D.R. Cheng, Y. Liu, S. Alberti, M. Dovizio, R. Landolfi, L. Mucci, P.-Z. Miao, P. Gao, D.-L. Zhu, J. Wang, B. Li, P. Patrignani, Y. Yu, Rare SNP rs12731181 in the miR-590-3p target site of the Prostaglandin F2α receptor gene confers risk for essential hypertension in the Han Chinese population, Arterioscler. Thromb. Vasc. Biol. 35 (2015) 1687–1695. doi:10.1161/atvbaha.115.305445.

[84] Y. Wang, S. Yan, B. Xiao, S. Zuo, Q. Zhang, G. Chen, Y. Yu, D. Chen, Q. Liu, Y. Liu, Y. Shen, Y. Yu, Prostaglandin F 2α facilitates hepatic glucose production through CaMKIIγ/p38/FOXO1 signaling pathway in fasting and obesity, Diabetes. 67 (2018) 1748–1760. doi:10.2337/db17-1521.

[85] P. Kaur, M.D. Reis, G.R. Couchman, S.N. Forjuoh, J.F. Greene, Jr, A. Asea,

SERPINE 1 links obesity and diabetes: a pilot study, J. Proteomics Bioinform. 3 (2010) 191. doi:10.4172/jpb.1000139.

[86] G.M. Coudriet, J. Stoops, A.V. Orr, B. Bhushan, K. Koral, S. Lee, D.M. Previte, H.H. Dong, G.K. Michalopoulos, W.M. Mars, J.D. Piganelli, A Noncanonical role for plasminogen activator inhibitor type 1 in obesity-induced diabetes, Am. J. Pathol. 189 (2019) 1413–1422. doi:10.1016/j.ajpath.2019.04.004.

[87] C.-S. Kuo, J.-S. Chen, L.-Y. Lin, G.W. Schmid-Schönbein, S. Chien, P.-H. Huang, J.-W. Chen, S.-J. Lin, Inhibition of serine protease activity protects against high fat diet-induced inflammation and insulin resistance, Sci. Reports. 10 (2020) 1–11. doi:10.1038/s41598-020-58361-4.

[88] J. Kosacka, M. Nowicki, S. Paeschke, P. Baum, M. Blüher, N. Klö ting, Up-regulated autophagy: as a protective factor in adipose tissue of WOKW rats with metabolic syndrome, Diabetol. Metab. Syndr. 10 (2018) 13. doi:10.1186/S13098-018-0317-6.

[89] J. Perttilä, K. Merikanto, J. Naukkarinen, I. Surakka, N.W. Martin, K. Tanhuanpää, V. Grimard, M.-R. Taskinen, C. Thiele, V. Salomaa, A. Jula, M. Perola, I. Virtanen, L. Peltonen, V.M. Olkkonen, OSBPL10, a novel candidate gene for high triglyceride trait in dyslipidemic Finnish subjects, regulates cellular lipid metabolism, J. Mol. Med. 2009 878. 87 (2009) 825–835. doi:10.1007/S00109-009-0490-Z.

[90] R.F. Bowen, N.S. Raikwar, L.K. Olson, M.A. Deeg, Glucose and insulin regulate glycosylphosphatidylinositol-specific phospholipase D expression in islet beta cells, Metabolism. 50 (2001) 1489–1492. doi:10.1053/meta.2001.28087.

[91] S. Ussar, O. Bezy, M. Blüher, C.R. Kahn, Glypican-4 enhances insulin signaling via interaction with the insulin receptor and serves as a novel adipokine,

Diabetes. 61 (2012) 2289–2298. doi:10.2337/db11-1395.

[92] J. Xu, X. Bao, Z. Peng, L. Wang, L. Du, W. Niu, Y. Sun, Comprehensive analysis of genome-wide DNA methylation across human polycystic ovary syndrome ovary granulosa cell, Oncotarget. 7 (2016) 27899. doi:10.18632/oncotarget.8544.

[93] F. Yeung, C.M. Ramírez, P.A. Mateos-Gomez, A. Pinzaro, G. Ceccarini, S. Kabir, C. Fernández-Hernando, A. Sfeir, Nontelomeric role for Rap1 in regulating metabolism and protecting against obesity, Cell Rep. 3 (2013) 1847–1856. doi:10.1016/j.celrep.2013.05.032.

[94] P. Martínez, G. Gómez-López, F. García, E. Mercken, S. Mitchell, J.M. Flores, R. de Cabo, M.A. Blasco, RAP1 protects from obesity through its extratelomeric role regulating gene expression, Cell Rep. 3 (2013) 2059–2074. doi:10.1016/j.celrep.2013.05.030.

[95] W. Yang, T. Kelly, J. He, Genetic epidemiology of obesity, Epidemiol. Rev. 29 (2007) 49–61. doi:10.1093/epirev/mxm004.

[96] Y. Zhou, L. Rui, Leptin signaling and leptin resistance, Front. Med. 7 (2013) 207–222. doi:10.1007/s11684-013-0263-5.

[97] A.G. Izquierdo, A.B. Crujeiras, F.F. Casanueva, M.C. Carreira, Leptin, obesity, and leptin resistance: where are we 25 years later?, Nutrients. 11 (2019) 2704. doi:10.3390/nu11112704.

Table 1: mRNA genes with the top 5% post-transcriptional (PTc) scores and at least 2-folds exonic fraction (ΔEx) reduction (equivalent to -1 in the $\log_2$ scale) from *gluteus medius* skeletal muscle expression profiles of fasting (*AL-T0*, N = 11) and fed (*AL-T2*, N = 12) Duroc gilts.

ID	Gene	$\log_2$FC	ΔEx	PT_c	*P*-value	*q*-value	DE	miRNA target
ENSSSCG00000032094	*DKK2*	-2.010	-1.431	-4.738	1.654E-05	3.830E-03	•	x
ENSSSCG00000015334	*PDK4*	-2.108	-5.250	-4.698	4.693E-03	1.330E-01	x	x
ENSSSCG00000015037	*IL18*	-1.655	-1.191	-3.682	4.787E-03	1.340E-01	•	x
ENSSSCG00000005385	*NR4A3*	-1.337	-3.082	-3.646	4.038E-02	4.098E-01	x	x
ENSSSCG00000003766	*DNAJB4*	-1.391	-1.008	-3.348	8.358E-03	1.905E-01		x
ENSSSCG00000015969	*CHRNA1*	-1.561	-1.339	-3.341	2.606E-03	9.406E-02	x	x
ENSSSCG00000039419	*SLCO4A1*	-1.055	-2.279	-3.180	2.820E-02	3.544E-01	x	x
ENSSSCG00000049158		-1.107	-1.096	-3.164	3.182E-02	3.735E-01		x
ENSSSCG00000004347	*FBXL4*	-1.298	-1.126	-3.133	1.422E-03	6.520E-02	x	x
ENSSSCG00000004979	*MYO9A*	-1.239	-1.003	-3.043	7.296E-03	1.731E-01		x
ENSSSCG00000013351	*NAV2*	-1.163	-1.196	-2.863	2.605E-04	2.301E-02	x	x
ENSSSCG00000032741	*TBC1D9*	-0.913	-1.061	-2.736	1.534E-02	2.583E-01	•	x
ENSSSCG00000031728	*ABRA*	-1.238	-1.393	-2.704	1.295E-03	6.116E-02	x	x
ENSSSCG00000006331	*PBX1*	-0.891	-1.039	-2.480	1.135E-02	2.177E-01	x	x
ENSSSCG00000035037	*SIK1*	-1.357	-1.289	-2.475	3.999E-03	1.212E-01	x	x
ENSSSCG00000038374	*CIART*	-1.027	-1.321	-2.052	1.543E-02	2.587E-01	x	
ENSSSCG00000023806	*LRRN1*	-0.776	-1.013	-1.983	1.580E-01	7.074E-01		x
ENSSSCG00000009157	*TET2*	-0.381	-1.123	-1.792	4.880E-01	9.582E-01		x
ENSSSCG00000011133	*PFKFB3*	-0.022	-2.256	-1.785	9.712E-01	9.987E-01	x	x
ENSSSCG00000002283	*FUT8*	-0.578	-1.286	-1.784	9.887E-02	6.059E-01	x	x
ENSSSCG00000023133	*OSBPL6*	-0.432	-1.088	-1.772	3.835E-01	9.108E-01	x	
ENSSSCG00000017986	*NDEL1*	-0.767	-1.644	-1.759	1.006E-02	2.081E-01	x	x
ENSSSCG00000031321	*NR4A1*	-0.630	-1.328	-1.720	6.298E-02	5.006E-01	x	
ENSSSCG00000035101	*KLF5*	-0.519	-1.487	-1.708	2.942E-01	8.488E-01	x	x
ENSSSCG00000004332	*BACH2*	-0.714	-2.105	-1.705	9.089E-02	5.861E-01	x	x
ENSSSCG00000017983	*PER1*	-0.773	-1.073	-1.627	3.000E-02	3.662E-01	x	

[a]$\log_2$FC: estimated $\log_2$ fold change for mean exonic fractions from *gluteus medius* expression profiles of fasted *AL-T0* and fed *AL-T2* Duroc gilts; [b]ΔEx: exonic fraction increment ($Ex_2 - Ex_1$) when comparing exon abundances in *AL-T0* (Ex_1) vs *AL-T2* (Ex_2) Duroc gilts; [c]PTc: post-transcriptional signal (ΔEx – ΔInt) in z-score scale; [d]q-value: q-value calculated with the false discovery rate (FDR) approach [40]. The "x" symbols represent differentially expressed (DE) genes (FC < -2; *q*-value < 0.05) according to their exonic fractions, as well as those targeted by at least one of the upregulated miRNAs excluding redundant seeds (N = 6, **Table S5**). The "•" symbol represents suggestive canonical differential expression (*P*-value < 0.01, **Table S4**).

Figure legends

Figure 1: (**A**) Scatterplot depicting mRNA genes with the top 5% negative PTc scores and at least 2-folds ΔEx reduction according to exonic (ΔEx) and PTc (ΔEx – ΔInt) values (in purple) and putatively targeted by DE upregulated miRNAs (FC > 1.5; *q*-value < 0.05) from *gluteus medius* skeletal muscle expression profiles of fasted (*AL-T0*, N = 11) and fed (*AL-T2*, N = 12) Duroc gilts. (**B**) Enrichment analyses of the number of mRNA genes with the top 5% negative PTc scores and at least 2-folds ΔEx reduction putatively targeted by DE upregulated miRNAs (FC > 1.5; *q*-value < 0.05), DE downregulated miRNAs (FC < -1.5; *q*-value < 0.05) and the top 5% most highly expressed miRNAs, excluding DE upregulated miRNAs. (**C**) Scatterplot depicting DE upregulated (in green) and downregulated (in red) mRNA genes (|FC| > 2; *q*-value < 0.05) according to exonic (ΔEx) and PTc (ΔEx – ΔInt) values. (**D**) Covariation enrichment scores (CES) for the exonic and intronic fractions of mRNA genes with the top 5% negative PTc scores and at least 2-folds ΔEx reduction, putatively targeted by upregulated miRNAs from *gluteus medius* skeletal muscle expression profiles of fasted (*AL-T0*, N = 11) and fed (*AL-T2*, N = 12) Duroc gilts. The control set of CES values were generated by permuted (N = 1,000) random sets of exonic and intronic profiles of genes with same size as those used before (N = 21). Significant differences were assessed using a Mann-Whitney U non-parametric test [48].

Figure 2: (**A**) Scatterplot depicting mRNA genes with the top 5% negative PTc scores and at least 2-folds ΔEx reduction according to exonic (ΔEx) and PTc (ΔEx – ΔInt) values (in purple) and putatively targeted by upregulated miRNAs (FC > 1.5; *P*-value < 0.01) from adipocyte expression profiles of *lean* (N = 5) and *obese* (N = 5) Duroc-Göttingen minipigs according to their body mass index (BMI). (**B**) Enrichment analyses

of the number of mRNA genes with the top 5% negative PTc scores and at least 2-folds ΔEx reduction putatively targeted by DE upregulated miRNAs (FC > 1.5; *q*-value < 0.05), DE downregulated miRNAs (FC < -1.5; *q*-value < 0.05) and the top 5% most highly expressed miRNAs, excluding DE upregulated miRNAs. (**C**) Scatterplot depicting DE upregulated (in green) and downregulated (in red) mRNA genes (|FC| > 2; *q*-value < 0.05) according to exonic (ΔEx) and PTc (ΔEx – ΔInt) values. (**D**) Covariation enrichment scores (CES) for the exonic and intronic fractions of mRNA genes with the top 5% negative PTc scores and at least 2-folds ΔEx reduction, putatively targeted by upregulated miRNAs from adipocyte expression profiles of *lean* (N = 5) and *obese* (N = 5) Duroc-Göttingen minipigs. The control set of CES values were generated by permuted (N = 1,000) random sets of exonic and intronic profiles of genes with same size as those used before (N = 25). Significant differences were assessed using a Mann-Whitney U non-parametric test [48]. (**E**) Barplots depicting qPCR $\log_2$ transformed relative quantities (Rq) for *LEP*, *OSBPL10*, *PRSS23*, *RNF157* and *SERPINE2* mRNA transcripts measured in adipocytes from the retroperitoneal fat of *lean* (N = 5) and *obese* (N = 5) Duroc-Göttingen minipigs. (**F**) Barplots depicting qPCR $\log_2$ transformed relative quantities (Rq) for ssc-miR-148a-3p, ssc-miR-214-3p and ssc-miR-92b-3p miRNA transcripts measured in the isolated adipocytes from the retroperitoneal fat of *lean* (N = 5) and *obese* (N = 5) Duroc-Göttingen minipigs.

Supplementary Tables

Table S1: Phenotype values for selected Duroc-Göttingen minipigs from the F2-UNIK resource population according to their body mass indexes (BMI).

Table S2: Primers for qPCR validation of selected mRNA and miRNA genes according to EISA results in the F2-UNIK Duroc-Göttingen minipig population comparing *lean* (N = 5) and *obese* (N = 5) individuals.

Table S3: Raw Cq values from qPCR analyses after efficiency correction measuring adipocyte expression profiles of selected mRNAs and miRNAs from *lean* (N = 5) and *obese* (N = 5) Duroc-Göttingen minipigs.

Table S4: Genes detected by *edgeR* tool as differentially expressed when comparing *gluteus medius* expression profiles of fasted *AL-T0* (N = 11) and fed *AL-T2* (N = 12) Duroc gilts.

Table S5: microRNAs detected by *edgeR* tool as differentially expressed when comparing *gluteus medius* expression profiles of fasted *AL-T0* (N = 11) and fed *AL-T2* (N = 12) Duroc gilts.

Table S6: EISA results for post-transcriptional signals (PTc) detected in *gluteus medius* skeletal muscle expression profiles of fasted (*AL-T0*, N = 11) and fed (*AL-T2*, N = 12) Duroc gilts.

Table S7: Binding sites for differentially upregulated miRNAs found in mRNA genes with the top 5% negative PT_c scores and at least 2-folds reduction in the exonic fraction (ΔEx) of *gluteus medius* skeletal muscle expression profiles from fasting (*AL-T0*, N = 11) and fed (*AL-T2*, N = 12) Duroc gilts.

Table S8: Covariation enrichment scores (CES) for the exonic and intronic fractions of mRNA genes with the top 5% negative post-transcriptional signals (PTc) and at least 2-folds reduction in their exonic (ΔEx) fraction, that were putatively targeted by DE upregulated miRNAs from *gluteus medius* skeletal muscle expression profiles *AL-T0 vs AL-T2* Duroc gilts (N = 21).

Table S9: Genes detected by *edgeR* tool as differentially expressed when comparing adipocyte expression profiles from *lean* (N = 5) and *obese* (N = 5) Duroc-Göttingen minipigs according to their body mass index (BMI).

Table S10: microRNA genes detected by *edgeR* tool as differentially expressed when comparing adipocyte expression profiles from *lean* (N = 5) and *obese* (N = 5) Duroc-Göttingen minipigs according to their body mass index (BMI).

Table S11: mRNA genes with the top 5% post-transcriptional signals (PTc) and at least 2-fold exonic fraction (ΔEx) reduction (equivalent to -1 in the log2 scale) from adipocyte expression profiles of lean (N = 5) and obese (N = 5) Duroc-Göttingen minipigs according to their body mass index (BMI).

Table S12: EISA results for post-transcriptional signals (PTc) detected in adipocyte expression profiles of *lean* (N = 5) and *obese* (N = 5) Duroc-Göttingen minipigs according to their body mass index (BMI).

Table S13: Binding sites for differentially upregulated miRNAs found in mRNA genes with the top 5% negative PTc scores and at least 2-folds reduction in the exonic fraction (ΔEx) of adipocyte expression profiles from *lean* (N = 5) and *obese* (N = 5) Duroc-Göttingen minipigs according to their body mass index (BMI).

Table S14: Covariation enrichment scores (CES) for the exonic and intronic fractions of mRNA genes with the top 5% negative post-transcriptional signals (PTc) and at least 2-folds reduction in their exonic (ΔEx) fraction, that were putatively targeted by DE upregulated miRNAs from adipocyte expression profiles of *lean* vs *obese* Duroc-Göttingen minipigs (N = 25).

Supplementary Figures

Figure S1: Diagram depicting the consecutive steps implemented for studying miRNA-driven post-transcriptional regulatory signals applying the EISA approach and additional enrichment and covariation analyses.

Figure S2: Scatterplots depicting the exonic (ΔEx) and intronic (ΔInt) fractions from *gluteus medius* skeletal muscle expression profiles of fasting (*AL-T0*, N = 11) and fed (*AL-T2*, N = 12) Duroc gilts. (**A**) mRNA genes with the top 5% post-transcriptional (PTc) negative scores and at least 2-folds reduced exonic (ΔEx) fractions (equivalent to -1 in the $\log_2$ scale), suggestive of miRNA-driven post-transcriptional regulation. (**B**) mRNA genes differentially expressed showing upregulation (FC > 2; *q*-value < 0.05, in green) and downregulation (FC < -2, *q*-value < 0.05, in red) in fed (*AL-T2*, N = 12) Duroc gilts with respect to their fasted (*AL-T0*, N = 11) counterparts.

Figure S3: Enrichment analyses of the number of genes with the (**A**) top 1% and (**B**) top 5% negative PTc scores and at least 2-fold reduced exonic fractions (ΔEx) putatively targeted by upregulated miRNAs (FC > 1.5; *q*-value < 0.05) from *gluteus medius* skeletal muscle expression profiles of fasting (*AL-T0*, N = 11) and fed (*AL-T2*, N = 12) Duroc gilts. Results show the change in enrichment significance when incorporating context-based pruning of miRNA binding sites of type 8mer, 7mer-m8 and 7mer-A1. R: Raw enrichment analyses without any additional context-based pruning. AU: Enrichment analyses removing miRNA binding sites without AU-rich flanking sequences (30 nts upstream and downstream). M: Enrichment analyses removing miRNA binding sites located in the middle of the 3'-UTR sequence (45-55%). E: Enrichment analyses removing miRNA binding sites located too close (< 15 nts) to the beginning or the end of the 3'-UTR sequences. The black dashed line represents a *P*-value = 0.05.

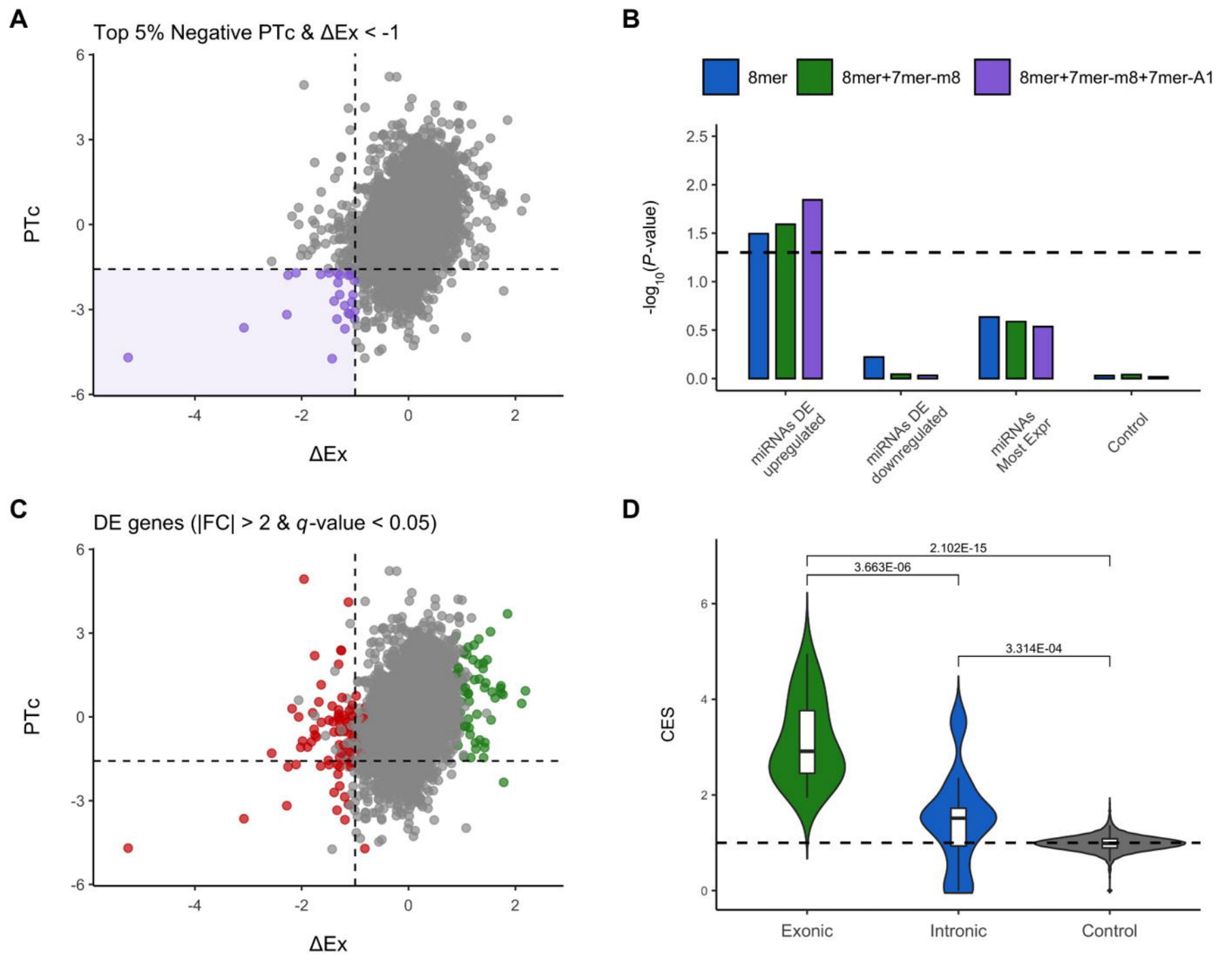
A
Top 5% Negative PTc & ΔEx < -1
PTc
ΔEx
B
8mer
8mer+7mer-m8
8mer+7mer-m8+7mer-A1
-log10(P-value)
miRNAs DE upregulated
miRNAs DE downregulated
miRNAs Most Expr
Control
C
DE genes (|FC| > 2 & q-value < 0.05)
PTc
ΔEx
D
2.102E-15
3.663E-06
3.314E-04
CES
Exonic
Intronic
Control

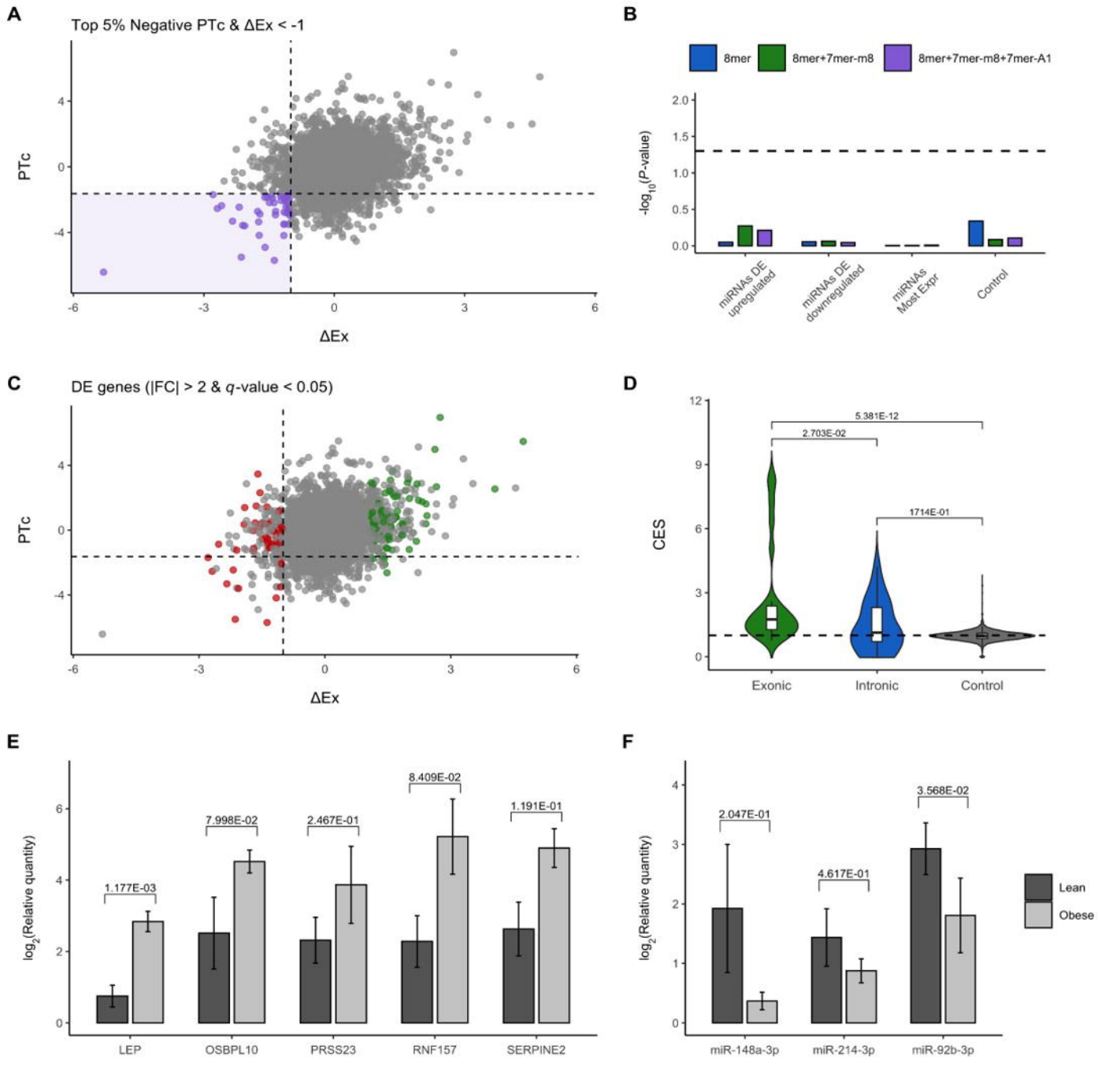
A
Top 5% Negative PTc & ΔEx < -1
PTc
ΔEx
B
8mer
8mer+7mer-m8
8mer+7mer-m8+7mer-A1
-log10(P-value)
miRNAs DE upregulated
miRNAs DE downregulated
miRNAs Most Expr
Control
C
DE genes (|FC| > 2 & q-value < 0.05)
PTc
ΔEx
D
CES
5.381E-12
2.703E-02
1714E-01
Exonic
Intronic
Control
E
log2(Relative quantity)
1.177E-03
7.998E-02
2.467E-01
8.409E-02
1.191E-01
LEP
OSBPL10
PRSS23
RNF157
SERPINE2
F
log2(Relative quantity)
2.047E-01
4.617E-01
3.568E-02
miR-148a-3p
miR-214-3p
miR-92b-3p
Lean
Obese